

UNIVERSITY OF CALIFORNIA

Los Angeles

# Cooperative Resource Allocation in Wireless Systems

A dissertation submitted in partial satisfaction of the  
requirements for the degree Doctor of Philosophy  
in Electrical Engineering

by

Seung Ryul Yang

2010

© Copyright by  
Seung Ryul Yang  
2010

The dissertation of Seung Ryul Yang is approved.

---

Kung Yao

---

Richard D. Wesel

---

John W. Wallace

---

Gregory J. Pottie, Committee Chair

University of California, Los Angeles

2010

# Contents

<b>1</b>	<b>Introduction</b>	<b>1</b>
<b>2</b>	<b>Background</b>	<b>4</b>
2.1	Wireless Channels . . . . .	4
2.2	Wireless Network Systems . . . . .	6
2.2.1	Ad-hoc Network Systems . . . . .	6
2.2.2	Cellular Network Systems . . . . .	8
2.3	Multi-user Wireless Systems . . . . .	10
2.3.1	Frequency Division Multiple Access (FDMA) . . . . .	11
2.3.2	Time Division Multiple Access (TDMA) . . . . .	11
2.3.3	Code Division Multiple Access (CDMA) . . . . .	13
2.3.4	Orthogonal Frequency Division Multiple Access (OFDMA) . . . . .	14
<b>3</b>	<b>On the Reduction of Relay Node Density with Cooperative Com- munication</b>	<b>17</b>
3.1	Introduction . . . . .	17
3.2	Simulation Model . . . . .	19
3.2.1	Basic Principles . . . . .	19
3.2.2	Proposed Power Cost for Cooperation . . . . .	21

3.2.3	Assumptions and Conditions for Simulation . . . . .	22
3.2.4	Channel Knowledge at the Transmitting Nodes . . . . .	24
3.2.5	Channel Models . . . . .	25
3.3	Simulation Results . . . . .	27
3.3.1	Path Diversity . . . . .	31
3.3.2	Non-uniformity . . . . .	34
3.4	Conclusion . . . . .	40
<b>4</b>	<b>Cooperative Power Control with Fast Convergence</b>	<b>41</b>
4.1	Introduction . . . . .	41
4.2	System Model . . . . .	43
4.2.1	Distributed Power Control . . . . .	44
4.3	Cooperative Power Control . . . . .	45
4.3.1	Cooperative Power Control Algorithm . . . . .	45
4.3.2	Convergence . . . . .	47
4.3.3	Convergence Speed . . . . .	49
4.4	Simulation Results . . . . .	50
4.5	Conclusion . . . . .	51
<b>5</b>	<b>Dynamic Resource Allocation with Low Complexity for Real Time Traffic in Uplink OFDMA Systems</b>	<b>56</b>
5.1	Introduction . . . . .	56
5.2	System Model and Problem Formulation . . . . .	58
5.3	Proposed Algorithm . . . . .	59
5.3.1	Power Allocation . . . . .	61
5.3.2	Subcarrier Allocation . . . . .	61
5.3.3	Complexity . . . . .	62

5.4	Simulation Results . . . . .	63
5.5	Conclusion . . . . .	64
<b>6</b>	<b>Conclusion and Future Works</b>	<b>67</b>
6.1	Conclusion . . . . .	67
6.2	Future Works . . . . .	68
<b>A</b>	<b>APPENDIX for Proofs of Theorems</b>	<b>70</b>
A.1	Proof of Theorem 1 . . . . .	70
A.2	Proof of Theorem 2 . . . . .	70
A.3	Proof of Theorem 3 . . . . .	71
	<b>Bibliography</b>	<b>73</b>

# List of Figures

2.1	Wireless ad-hoc network . . . . .	7
2.2	Wireless ad-hoc network with multi-hopping . . . . .	7
2.3	Hexagonal cellular pattern with reuse factor 1 . . . . .	9
2.4	Hexagonal cellular pattern with reuse factor 1/3 . . . . .	9
2.5	Hexagonal cellular pattern with reuse factor 1/7 . . . . .	10
2.6	An illustration of radio resource distribution of multiple access schemes	16
3.1	A non-cooperative and cooperative relay with different required node densities for the same quality . . . . .	19
3.2	Required node density vs. achievable rate . . . . .	23
3.3	Reduction of node density in non-fading channels . . . . .	27
3.4	Reduction of node density in random Rayleigh fading channels . . . . .	28
3.5	Reduction of node density in quasi-static Rayleigh fading channels . . . . .	29
3.6	Required node density in random Ricean channels . . . . .	32
3.7	Reduction of node density in random Ricean channels . . . . .	33
3.8	The expected largest path gain with $\alpha = 2$ . . . . .	36
3.9	The expected values of the largest several path gains with $\alpha = 2$ . . . . .	37
3.10	Required node density in quasi-static Ricean channels with $\alpha = 2$ . . . . .	38
3.11	Reduction of node density in quasi-static Ricean channels with $\alpha = 2$ . . . . .	39

4.1	Cooperative Groups and Distributed (Non-cooperative) links (cells or P2P pairs) . . . . .	46
4.2	The number of iterations with cooperation . . . . .	52
4.3	The maximum modulus eigenvalue with cooperation . . . . .	53
4.4	The overall latency with cooperation . . . . .	54
5.1	Average outage probability . . . . .	65
5.2	Maximum outage probability . . . . .	66

# List of Tables

2.1	Path attenuation factors for different environments . . . . .	5
2.2	Standard deviation $\sigma$ (in dB) for the wideband microcell model at 1900MHz of line-of-sight (LOS) and obstructed (OBS) environments .	5
3.1	Examples for the number of possible routes . . . . .	30
5.1	Proposed URA algorithm . . . . .	62
5.2	A protocol for distributed implementation of the proposed URA algorithm . . . . .	63

# Acknowledgments

I would like to express my greatest gratitude to my advisor Gregory J. Pottie for his guidance and assistance. He is always motivating and inspiring me and our research group. When I was faced with hardships, I was able to draw strength from his encouraging with the great efforts and concerns. I am in great respect for his passion, brilliance, discretion and positiveness as a research and a person as well.

I would like also to thank the other members of my dissertation committee: Dr. Kung Yao, Dr. Richard D. Wesel, and Dr. John W. Wallace. I am grateful to all my teachers at UCLA for providing intellectual backgrounds to me.

To my family, I would like to thank them for their supports and sacrifices. I could not have done anything without them. I would finally like to thank my baby son, Nathan. I am extremely lucky to have him in my life.

# VITA

January 10, 1978	Born, Seoul, Korea
2002-04	Simulation Programmer OFDM system Test-bed, Korea University Seoul, Korea
2004	B.A., Eletrical Engineering Korea University Seoul, Korea
2006	M.S., Eletrical Engineering University of California, Los Angeles Los Angeles, California
2006, 09	Teaching Assistant Department of Eletrical Engineering University of California, Los Angeles
2006 ~ 08	Research Assistant Center for Embedded Networks Systems (CENS) University of California, Los Angeles
2008 ~ 10	Research Assistant Department of Eletrical Engineering University of California, Los Angeles

# ABSTRACT OF THE DISSERTATION

Cooperative Resource Allocation in Wireless Systems

by

Seung Ryul Yang

Doctor of Philosophy in Electrical Engineering

University of California, Los Angeles, 2010

Professor Gregory J. Pottie, Chair

Strategies to improve network capacities of ad-hoc relay, power control, and orthogonal frequency division multiple access (OFDMA) systems are proposed. First, we examine how the node density can be reduced by cooperative actions of nodes in ad-hoc networks in multi-hop routing. This results from the greater channel capacity of the broadcast, multiple access and multiple-input multiple-output (MIMO) channel compared to the point-to-point channel for the individual links making up the paths. We simulate the effects of cooperative actions in various channel conditions under very optimistic assumptions to establish upper limits on the benefits of cooperation. In some circumstances, node density can be reduced by up to 80% although lesser gains are more typical. Second, we have devised a cooperative power control algorithm and proved that the cooperation enhances the convergence speed. The cooperative links predict the future interference state as reliably as possible with the shared information. This brings a significant improvement in the convergence speed. It is proved by the eigenvalue analysis that not all the cross-link gains in a cooperative group have to be identified and shared; using any of them reduces the maximum modulus eigenvalue of the matrix updating power vector. Finally, we proposed an efficient dynamic resource allocation algorithm for real time traffic in uplink OFDMA

systems. In contrast to the conventional algorithms performing computations for each subcarrier, the proposed algorithm performs computations for each user. Since the number of users who do not meet their quality-of-service (QoS) requirements is usually very small in practical situations, the proposed algorithm results in a large reduction in the complexity. In addition to the complexity reduction, the proposed algorithm outperforms the conventional algorithms for real time traffic.

# Chapter 1

## Introduction

Wireless communication systems have become pervasive, ranging from such simple functions as sending signals to open a garage door, to third generation cellular devices carrying a broad range of multimedia traffic. While wireless communication systems share many characteristics with wired systems, there are two distinguishing aspects. First, the channels are variable and generally unknown, with each link presenting different propagation losses. Second, it is inherently a multiple access medium. Many users compete for the same band of frequencies. Thus, management of the mutual interference of users to meet QoS requirements is a primary design objective. While there are multiple access wired systems, typically all users have the same propagation losses and a master controller can easily coordinate access. The situation is different in wireless systems. Since there can be significant cost in learning the channel conditions and sharing them, questions arise as to how the resources should be controlled. Our focus is on the costs and benefits of different degrees of cooperation among users and controllers in gathering and exchanging such channel and interference state information. As a beginning, Chapter 2 introduces background knowledge for this dissertation. The characteristics of wireless channels, ad-hoc network systems and cellular network systems, and various multiple access schemes for multi-user wireless

systems are briefly explained.

In Chapter 3, ad-hoc relay network systems are considered. In an ad-hoc network consisting of a source, destination and intermediate relaying nodes, the network capacity corresponds to the required number of relay nodes with a specific quality of the multi-hopping communication. Assuming a proper routing protocol is performed, a strategy is to increase the effective transmitting ranges of each hop. With cooperation of closely located nodes, each of them can act like a transmitting antenna of a MIMO system. Due to the improvement of achievable rate using the virtual MIMO technique, the effective transmitting range can be also increased. Therefore, fewer relay nodes are required for the same quality of communication between the source and destination nodes with cooperation compared to without cooperation. The reduction of relay node density for various channel conditions is determined by simulation, and the results are analyzed.

In Chapter 4, an algorithm for fast converging power control is proposed. As long as power control algorithms converge to the same solution, the network capacity of a power-controlled network can be determined by the speed of convergence. Even though the existing distributed power control algorithm is attractive due to the simplicity and stability, it has a drawback of convergence speed which is a critical issue for delay sensitive applications and when either the traffic or channel dynamics are fast. A cooperative power control algorithm is proposed. It is shown how much faster the cooperative algorithm converges than a distributed algorithm. The enhancement of the convergence speed of the cooperative algorithm is proved with eigenvalue analysis.

In Chapter 5, an efficient radio resource allocation algorithm is suggested for up-link orthogonal frequency division multiple access (OFDMA) systems. Even though the resource allocation algorithms have been widely investigated, most of them deal with downlink systems only and focus on maximizing sum rate or minimizing trans-

mitting power. In current network environments, real time media traffic is increasingly dominating. Thus, QoS requirements of real time traffic need to be given more attention. In uplink systems, due to the distributed nature of power constraints, a quite different approach from downlink systems is required. The proposed algorithm with a strategy of user-by-user allocation outperforms the conventional algorithms with remarkably reduced complexity for real time traffic in uplink OFDMA systems.

Finally, our conclusions are presented along with suggestions for future research in Chapter 6.

# Chapter 2

## Background

In this chapter we provide background on a number of topics required for understanding our results. We begin with the modeling of wireless links. We then discuss different network topologies and classical multiple access techniques.

### 2.1 Wireless Channels

Wireless communication simply refers to the transfer of information over a wireless channel without any wired infrastructure. The wireless channel is extremely unpredictable and hard to analyze. There are three major propagation components to characterize the wireless channel: path attenuation, shadowing and fading.

The received power tends to be attenuated as the communication distance increases,

$$P_{rx} \propto P_{tx} \cdot d^{-\alpha}, \tag{2.1}$$

where  $P_{rx}$  is the received power,  $P_{tx}$  is the transmitted power,  $d$  is the distance between the transmitter and receiver, and  $\alpha$  is the positive path attenuation factor (or propagation loss factor). The path attenuation factor  $\alpha$  depends on the specific propagation environment, and it is listed in Table 2.1 [1].

Table 2.1: Path attenuation factors for different environments

Environment	Path attenuation factor $\alpha$
Free space	2
Urban area cellular radio	2.7 ~ 3.5
Shadowed urban cellular radio	3 ~ 5
In building line-of-sight	1.6 ~ 1.8
Obstructed in building	4 ~ 6
Obstructed in factories	2 ~ 3

The average received powers with the same  $P_{tx}$  and  $d$  vary due to some propagation mechanisms such as reflection, diffraction, and scattering caused by various surrounding obstructions [1], [4]. This variation of the received power, called shadowing, is often modeled as a log-normal random variable  $X_s$  which is a zero-mean (in dB) Gaussian distributed random variable with standard deviation  $\sigma$  (in dB). An example for the standard deviation for an outdoor model is shown in Table 2.2 [1], [2]. Including the effect of shadowing, the received power is represented as

$$P_{rx} = GP_{tx}d^{-\alpha}X_s, \quad (2.2)$$

where  $G$  is a constant including the transmitter and receiver antenna gains, system loss factor, and so on.

Table 2.2: Standard deviation  $\sigma$  (in dB) for the wideband microcell model at 1900MHz of line-of-sight (LOS) and obstructed (OBS) environments

Transmitter antenna height	$\sigma$ with LOS	$\sigma$ with OBS
Low (3.7m)	8.76	9.31
Medium (8.5m)	7.88	7.67
High (13.3m)	8.77	7.94

The transmitted signals are combined at the receiver after passing through multiple paths, and the envelope of the combined received signal varies, called fading. Fading tends to change with time due to the mobility of transmitters, receivers, or surrounding obstructions. The characteristic of the time varying envelope is modeled as a Rayleigh (without LOS) or Ricean (with LOS) distributed random variable  $X$ . The probability density function (pdf) of the Rayleigh distribution is given by [1], [3]

$$f_X(x) = \begin{cases} \frac{x}{\sigma^2} \exp\left(-\frac{x^2}{2\sigma^2}\right), & 0 \leq x \leq \infty \\ 0, & x < 0 \end{cases}, \quad (2.3)$$

where  $\sigma^2$  is the time-average power of the received signal before envelope detection. The pdf of the Ricean distribution is given by [1]

$$f_X(x) = \begin{cases} \frac{x}{\sigma^2} \exp\left[-\frac{(x+A)^2}{2\sigma^2}\right] I_0\left(\frac{Ax}{\sigma^2}\right), & x \geq 0, A \geq 0 \\ 0, & x < 0 \end{cases}, \quad (2.4)$$

where  $A$  is the peak amplitude of the dominant signal and  $I_0(\cdot)$  is the modified Bessel function of the first kind and zero-order.

## 2.2 Wireless Network Systems

### 2.2.1 Ad-hoc Network Systems

A wireless ad-hoc network is a decentralized wireless network. Ad-hoc networks consist of a collection of mobile and static nodes without any preexisting infrastructure such as routers, access points or base stations (BSs) and centralized administration. The nodes are equipped with wireless transmitters and receivers, and communicate with each other in distributed ways (see Fig. 2.1).

Since the transmitters of the nodes have limited effective ranges, the nodes are capable of multi-hopping relay through intermediate nodes in order to communicate

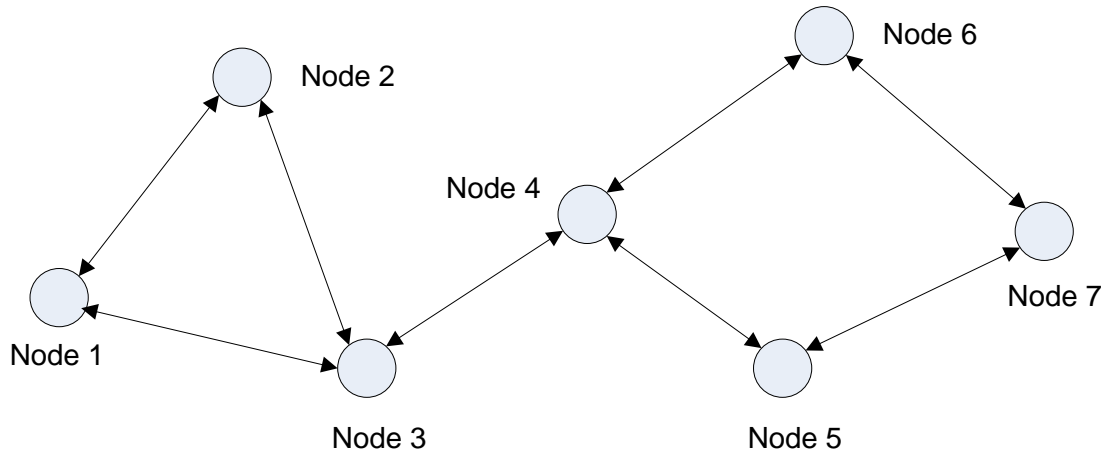


Figure 2.1: Wireless ad-hoc network

with their intended receiving nodes located further away than the effective ranges. That is, each node in the network acts as a transmitter, receiver and router (see Fig. 2.2). Therefore, the ad-hoc network is dynamically self-organizing and self-configuring with nodes establishing the necessary routing between each other without requirement for any existing infrastructure and administration [5]. Many routing protocols for ad-hoc network systems have been proposed. (See comprehensive surveys [6]–[8] and references therein.)

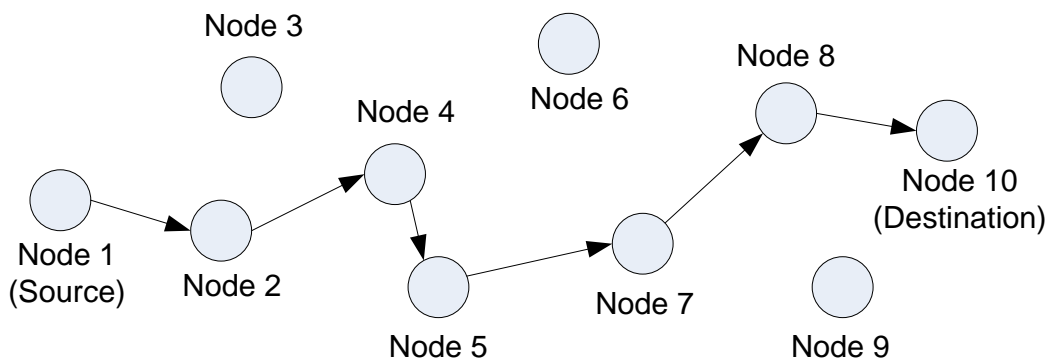


Figure 2.2: Wireless ad-hoc network with multi-hopping

Under particular assumptions on traffic distributions, the ad-hoc network capacity was found by P. Gupta and P. R. Kumar [9]. Some cooperative strategies are studied in [10], and a simulation study is shown in Chapter 3.

### 2.2.2 Cellular Network Systems

A wireless cellular network is a centralized wireless network with preexisting infrastructure and centralized administration. The coverage area is divided into smaller areas, *cells*. The cellular network systems allow nodes to communicate only within cells (specifically with a base station (BS) which is located near center of its cell) and the communication distances in the cellular network systems are confined under the cell radius in contrast to the ad-hoc network systems. Thus multi-hopping and routing protocols are not required, and the transmitting power can be economized in the cellular network systems.

The intra-cell interference is managed to be acceptable with various multiple access schemes, but a problem of the inter-cell interference (ICI) may remain even though it is limited by the cell radius. The ICI can be controlled by various frequency reuse patterns [4]. The frequency reuse patterns with the reuse factor 1, 1/3 and 1/7 are illustrated in Figs. 2.3, 2.4, and 2.5 respectively. The ICI can be bounded by allowing only a limited number of frequency bands for each cell. Due to the randomness of wireless channels caused by such factors as shadowing and fading, frequency re-use only gives a statistical bound on ICI.

Many other strategies and algorithms to control ICI, and thus improve the cellular network capacity, have been proposed such as power control, frequency reuse factor control and radio resource allocation. Power control and radio resource allocation problems are dealt with in Chapter 4 and 5 respectively.

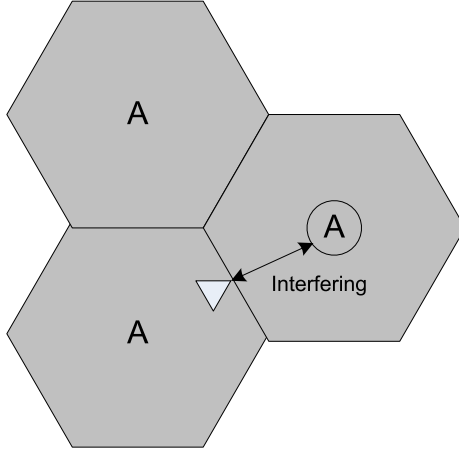


Figure 2.3: Hexagonal cellular pattern with reuse factor 1

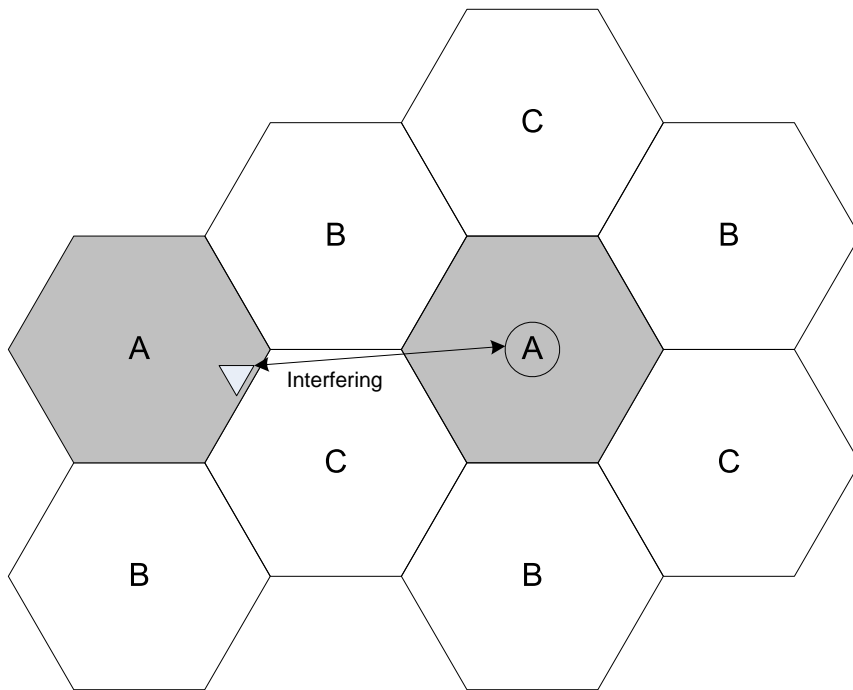


Figure 2.4: Hexagonal cellular pattern with reuse factor  $1/3$

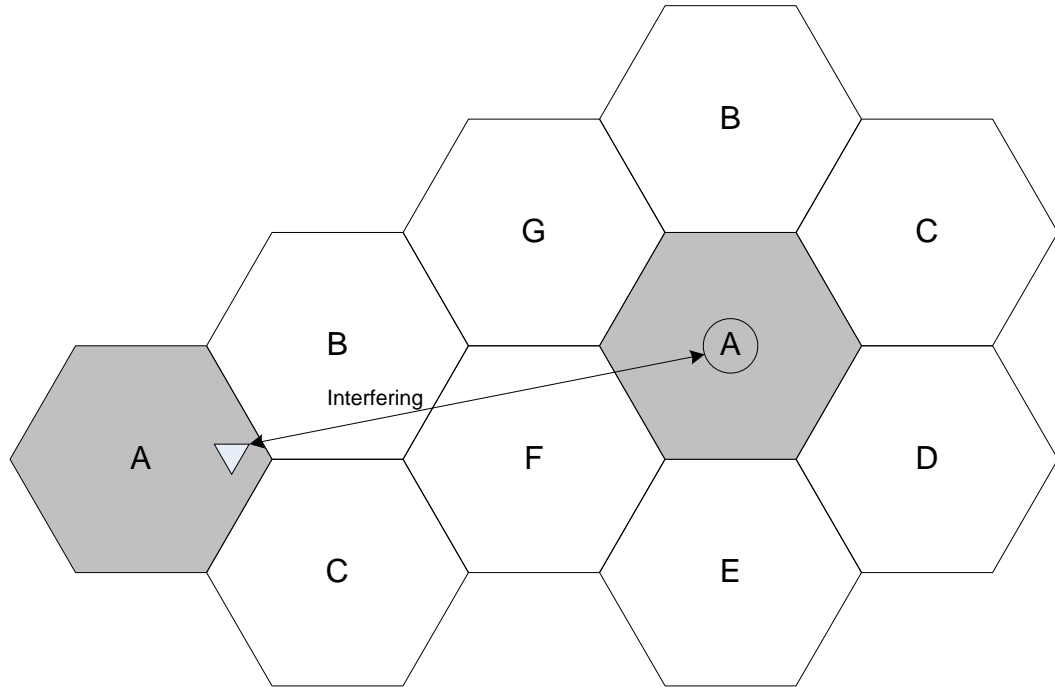


Figure 2.5: Hexagonal cellular pattern with reuse factor  $1/7$

## 2.3 Multi-user Wireless Systems

In wireless communication systems, multiple users are usually located closely (within others transmission ranges), and may interfere with each other severely. Therefore, protocols for wireless multi-user systems are required so that those users coexist such that they obtain enough radio resources to satisfy their QoS requirements. The design protocols for multi-user access in wireless systems is one of the most important research issues due to the increasing demands of wireless communications requiring high QoS in the limited radio resource. Many multiple access schemes have been investigated in order to reduce interference among them and, thus, improve network capacity. Some popular multiple access schemes, TDMA, CDMA, FDMA and OFDMA, are introduced here.

### 2.3.1 Frequency Division Multiple Access (FDMA)

FDMA divides the radio resource into non-overlapped frequency bands. The non-overlapped frequency bands are exclusively allocated to users in a FDMA system. Therefore, there is almost no interference caused among users with well designed filtering.

FDMA is used in the 1st generation (1G) wireless systems such as Advanced Mobile Phone System (AMPS), and Cordless Telephone (CT2), Digital European Cordless Telephone (DECT), and so on.

The advantages and disadvantages of FDMA are as follows [1]:

- Advantages

- The amount of inter-symbol interference is low and, thus, little or no equalization is required since FDMA is usually implemented in narrow band systems.
- The system complexity and overhead for synchronization is low compared to TDMA.

- Disadvantages

- Costly bandpass filters are required.
- Duplexers are required since both the transmission and reception operate at the same time.
- Tight RF filtering is required to minimize adjacent channel interference.

### 2.3.2 Time Division Multiple Access (TDMA)

TDMA divides the radio resource into non-overlapped time slots. The non-overlapped time slots are exclusively allocated to users in a TDMA system. Therefore, there is

no interference caused among the users while the same frequency bands can be shared by many users.

TDMA is used in 2G wireless systems such as Global System for Mobile Communications (GSM), IS-136, Personal Digital Cellular (PDC), Integrated Digital Enhanced Network (iDEN), and in the Digital Enhanced Cordless Telecommunications (DECT) standard for portable phones. It is also used extensively in satellite systems, and combat-net radio systems.

The advantages and disadvantages of TDMA are as follows [1]:

- Advantages

- Battery can live longer since the transmissions are not time-continuous and they can be turned off when not in use.
- The hand-off process is simple since it is able to listen for other BSs during idle time slots.
- Duplexers are not required since users use different time slots for transmission and reception.
- The bandwidth can be supplied on demand to different users since it is possible to allocate different numbers of time slots per frame to different users.

- Disadvantages

- Adaptive equalization is usually necessary since users are assigned short time slots and the transmission rates are generally very high.
- The guard time should be minimized.
- High time synchronization overhead is required due to the burst transmission.

### 2.3.3 Code Division Multiple Access (CDMA)

CDMA assigns users to distinct codes while all users share the total radio resource of a network such as frequency bands and time slots. CDMA employs spread-spectrum technology and a special coding scheme. The code is usually a pseudo-noise (PN) sequence with low cross correlation, and the signal appears noise-like to non-intended receivers. Since the interference is spread over a large spectrum and affects other users like background noise, many users can share the same radio resource with little coordination. CDMA systems are usually categorized into direct sequence CDMA (DS-CDMA) and frequency hopped CDMA (FH-CDMA).

CDMA is used in 2G and 3G wireless systems such as US narrowband spread Spectrum (IS-95), W-CDMA (3GPP), cdma2000 (3GPP2), and so on.

The advantages and disadvantages of CDMA are as follows [1]:

- Advantages

- CDMA has a soft capacity limit and there is no absolute limit on the number of users even though the system performance gradually degrades as the number of users is increased.
- Multi-path fading may be substantially reduced since the signal is spread over a large spectrum.
- Soft hand-off is performed whereby each user can be monitored by multiple BSs, and fewer users are dropped compared to the traditional hand-off procedures.

- Disadvantages

- Self-jamming arises from the fact that the spreading sequences of different users are not exactly orthogonal.

- The near-far problem occurs at a CDMA receiver if an undesired user has a high detected power as compared to the desired user.

### **2.3.4 Orthogonal Frequency Division Multiple Access (OFDMA)**

OFDMA divides the radio resource into overlapped but orthogonal frequency bands. The orthogonal frequency bands (not necessarily single and adjacent) are exclusively allocated to users and users transmit signals on the assigned subcarriers. The data of each user is divided into several parallel data streams and modulated on the multiple subcarriers allocated to the user in an OFDMA system. Due to the orthogonality, there is almost no interference caused among users with well designed filtering and acceptable frequency offset. Moreover, differing numbers of subcarriers can be allocated to users depending on their QoS requirements.

OFDMA is popularly used in 4G wireless systems of wideband communications such as Worldwide Interoperability for Microwave Access (WiMAX), 3GPP Long Term Evolution (LTE), and Evolved UMTS Terrestrial Radio Access (E-UTRA), a candidate access method for the IEEE 802.22 Wireless Regional Area Networks (WRAN), and so on.

The advantages and disadvantages of OFDMA are as follows [11]:

- Advantages
  - High frequency efficiency can be achieved since overlapped frequency bands are allocated for users.
  - Simple equalization is possible since the subcarriers are narrow enough to be assumed flat.

- ISI can be removed easily by guard intervals since the symbol duration on each subcarrier can be longer than for single-tone modulation schemes.
- Implementation is efficient using inverse fast Fourier transform (IFFT) and fast Fourier transform (FFT).
- Radio resource can be allocated easily to users on demand since different numbers of subcarriers can be allocated to different users.
- Disadvantages
  - Performance is sensitive to the frequency offset caused by Doppler shift or frequency synchronization in order to maintain the orthogonality among the subcarriers.
  - Linear transmitter circuitry is required due to the high peak-to-average-power ratio (PAPR).
  - Efficiency is reduced by the guard intervals.

In this dissertation, unless stated otherwise, we will generally be assuming the multiple access scheme to be OFDMA, due to its orthogonality within cells and its flexibility for resource allocation.

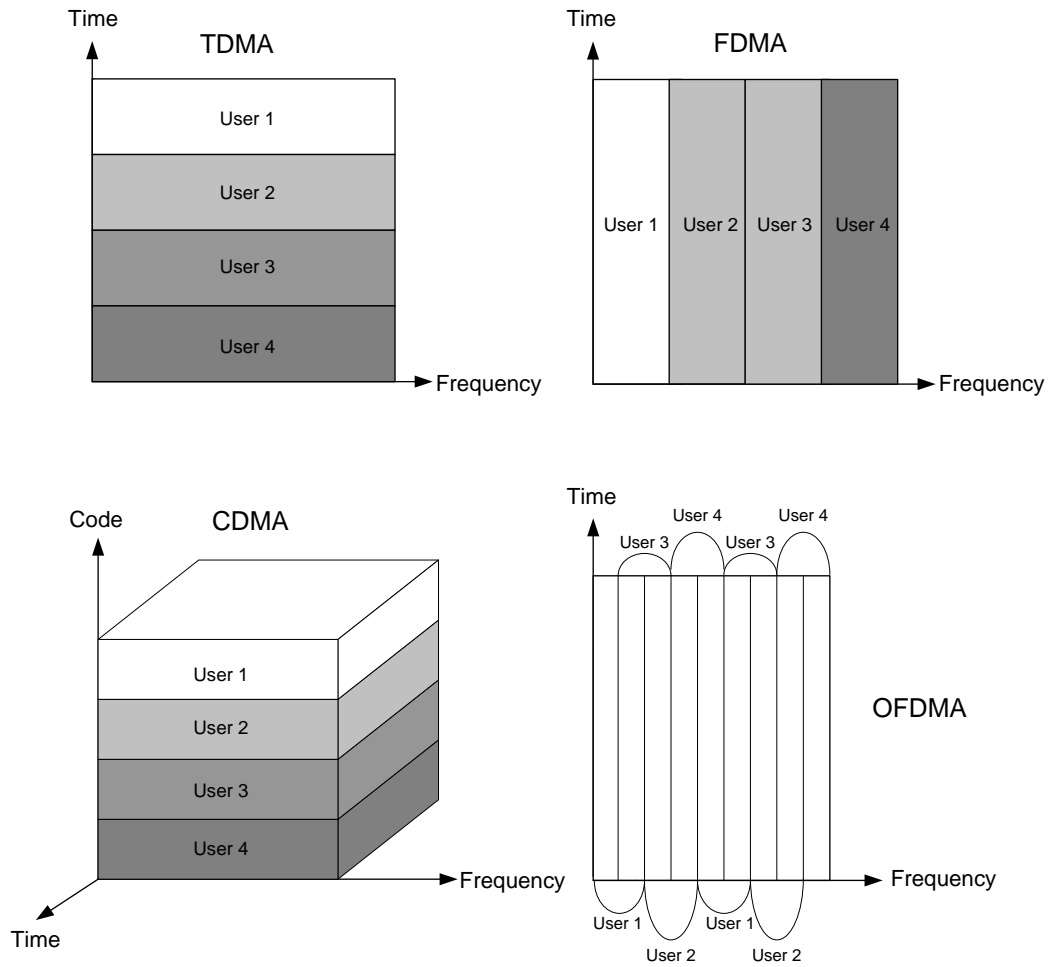


Figure 2.6: An illustration of radio resource distribution of multiple access schemes

# Chapter 3

## On the Reduction of Relay Node Density with Cooperative Communication

### 3.1 Introduction

Single antenna transmitters/receivers having size, cost, or hardware limitations for the multiple-antennas equipment in a multi-user environment can share their antennas and generate virtual MIMO systems with their cooperative actions called cooperative communication [10]. Since the work of T. Cover and A. Gamal on the concept of relaying [12], many cooperation techniques have been proposed such as decode-and-forward (DF) and amplify-and-forward (AF) [13]–[16], compress-and-forward (CF) signaling [17], coded cooperation [18], [19], space-time coded cooperation [20], [21], collaborative beam-forming [22], [23], asynchronous cooperation [24]–[26], and cross-layered approaches [23], [27].

Cooperative communication within ad-hoc networks increases the QoS between

nodes since the multiple-input multiple-output (MIMO) systems have the advantage of the single-input single-output (SISO) systems in the achievable rate, bit error rate, block error rate or outage probability by their spatial multiplexing gain [28]. Accordingly the cooperative transmitters and/or receivers can communicate through a longer distance than can a non-cooperative transmitter and receiver with the same quality. Equivalently, a smaller number of relay nodes can guarantee the same quality by their cooperative actions within the same region. The focus of this chapter is on how much the required node density can be reduced by cooperation in the context of multi-hop routing. Since asymptotic results indicate that cooperation does not change non-scalability [9], there remains the question of by what constant factor can cooperation boost capacity. This is an attempt to answer whether it is worth trying to devise practical cooperative schemes. In some scenarios we consider, the answer is clearly no, while in others there may be significant benefits.

While it is well-known that optimal MIMO schemes can improve capacity in co-located transmitter and receiver sets, in ad-hoc networks there is a cost for cooperation, in the form of the exchange of information among the cooperatively transmitting nodes and receiving nodes (there is an additional infrastructure cost to supply synchronism which we do not consider). On the one hand we may get little benefit from cooperation due to the geographic spread of possible partners as compared to the distance to be traversed. On the other hand, in a multi-hop route one link may limit capacity and improving it may have a large benefit. Given the analytical difficulties, we proceed by means of simulation. In Section 3.2 we present our models, in Section 3.3 we present our simulation results and we conclude in Section 3.4.

## 3.2 Simulation Model

### 3.2.1 Basic Principles

For uniformly-randomly-distributed nodes including a source and destination in a disk (see Fig. 3.1), the minimum node density which guarantees communication above a desired rate with high probability ( $p \geq 0.9$ ) is evaluated in various channel conditions. Assuming encoding and decoding are performed at each node, the problem reduces to simple routing. The minimum achievable rate of each hop, which is defined as the direct communication between transmitting nodes and receiving nodes, can be seen as the achievable rate of a route no matter which cooperation models are selected in the route by minimum cut set theory [29], assuming no interference among the hops, i.e.,

$$R^j = \min_i R_i^j \geq r_d, \quad (3.1)$$

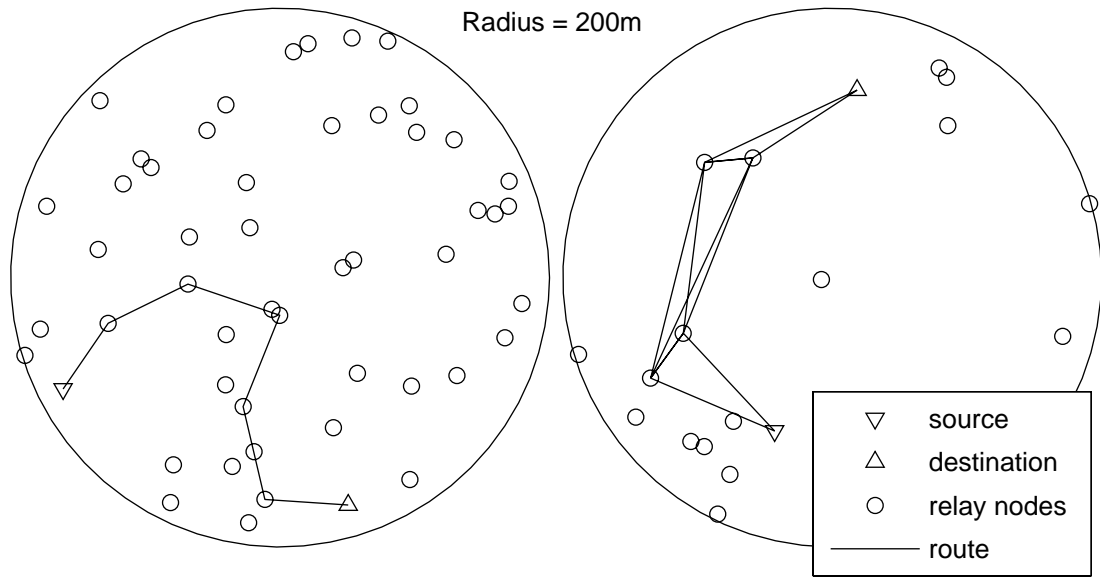


Figure 3.1: A non-cooperative and cooperative relay with different required node densities for the same quality

where  $R^j$  is the achievable rate of route  $j$ ,  $R_i^j$  is the achievable rate of the  $i$ th hop making up the route  $j$  and  $r_d$  is the desired rate.

The virtual  $M_T \times M_R$  MIMO channel with node cooperation can be modeled as

$$\mathbf{y} = \mathbf{H}\mathbf{x} + \mathbf{n}, \quad (3.2)$$

where  $M_T$  is the number of transmitting nodes,  $M_R$  is the number of receiving nodes,  $\mathbf{y} \in \mathbb{C}^{M_R}$  is the received signal vector,  $\mathbf{H}$  denotes the  $M_R \times M_T$  channel gain matrix,  $\mathbf{x} \in \mathbb{C}^{M_T}$  is the transmitted signal vector, and  $\mathbf{n}$  is the complex additive white Gaussian noise (AWGN) vector with zero mean and covariance matrix  $N_0\mathbf{I}_{M_R}$  where  $N_0$  is the additive noise power and  $\mathbf{I}_{M_R}$  is the  $M_R \times M_R$  identity matrix.

The achievable rate for a single hop with cooperation of nodes can be obtained from the mutual information [30], [31],

$$I(\mathbf{Q}) = \log_2 \det \left( \mathbf{I}_{M_R} + \frac{P_t}{M_T N_0} \mathbf{H}\mathbf{Q}\mathbf{H}^H \right), \quad (3.3)$$

where  $\mathbf{Q}$  is the input covariance matrix,

$$\mathbf{Q} = E[\mathbf{x}\mathbf{x}^H], \quad (3.4)$$

$P_t$  is the total transmitted power,  $(\cdot)^H$  denotes the conjugate transpose, and  $E(\cdot)$  is the expected value. Then the (ergodic) capacity of the MIMO channel for a deterministic channel is [28], [30]–[32]

$$C = \max_{\mathbf{Q}} I(\mathbf{Q}) \text{ b/s/Hz}. \quad (3.5)$$

For a random channel it is given by [28], [30]–[32]

$$C = \begin{cases} E_{\mathbf{H}} \left[ \max_{\mathbf{Q}} \{I(\mathbf{Q})\} \right] \text{ b/s/Hz,} & \text{perfect CSIR, CSIT} \\ \max_{\mathbf{Q}} \left[ E_{\mathbf{H}} \{I(\mathbf{Q})\} \right] \text{ b/s/Hz,} & \text{perfect CSIR only} \end{cases}, \quad (3.6)$$

where CSIR and CSIT stand for channel state information at receiving and transmitting nodes respectively. We assume the limited-peak-power constraint per node

which is more practical and needs cooperative action more than the limited-total-power constraint of nodes. The achievable rate for a single hop with a limited-peak power  $P_{lp}$  per node is given by the MIMO capacity in (3.5) and (3.6) obtained from the mutual information with  $P_{lp}$ ,

$$I(\mathbf{Q}) = \log_2 \det \left( \mathbf{I}_{M_R} + \frac{P_{lp}}{N_0} \mathbf{H} \mathbf{Q} \mathbf{H}^H \right), \quad (3.7)$$

where the diagonal elements of  $\mathbf{Q}$  are smaller than or equal to 1.

### 3.2.2 Proposed Power Cost for Cooperation

For cooperative transmission, the transmitting nodes must exchange their information before the hop [33] since they should share the information to be transmitted to the receiving nodes to get spatial multiplexing gain [28]. Thus the cooperatively transmitting partners are selected by the achievable rate between them since not only the rate of each hop but also the rate of exchanging the information of transmitting signals between them must exceed the desired rate in (3.1). That is, the nodes  $a$ ,  $b$ ,  $c$  and  $d$  can be cooperatively transmitting partners if

$$R_{ex}^i \geq r_d, \quad \text{for all } i \in S = \{a, b, c, d\}, \quad (3.8)$$

where  $R_{ex}^i$  is the achievable rate between any single node  $i$  and the others of the set  $S$ . The cooperatively transmitting nodes transmit signals to receiving nodes with the remaining power after their information exchange. We have

$$P_{tx}^i = P_{lp} - P_{ex}^i, \quad (3.9)$$

where the power cost for cooperation defined as

$$P_{ex}^i = \frac{N_0 \cdot (2^{R_{ex}^i} - 1)}{\mathbf{H}^H \mathbf{H}} = \frac{N_0 \cdot (2^{r_d} - 1)}{\mathbf{H}^H \mathbf{H}}, \quad (3.10)$$

$P_{tx}^i$  is the transmitted power of node  $i$  to receiving nodes,  $P_{ex}^i$  is the power of node  $i$  for  $R_{ex}^i$  and  $\mathbf{H}$  is the  $m \times 1$  channel matrix for  $m$  cooperatively transmitting partners of node  $i$ .

### 3.2.3 Assumptions and Conditions for Simulation

The main factors which determine the achievable rate of a hop are the channel conditions, cooperation order and power constraint. The channel conditions consist of the propagation loss, additive noise, scattering, shadowing and so on. The cooperation order is defined, in this chapter, as how many transmitting and receiving nodes cooperate with each other in each hop, i.e., cooperation-order  $k$  is defined as

$$k = \max \{M_T, M_R\}. \quad (3.11)$$

The cooperation-orders 2, 3 and 4 are considered in this chapter under the limited-peak-power constraint per node.

The required node densities with a fixed transmitted power for various achievable rates in non-fading channels are shown in Fig. 3.2. Since the achievable rate completely depends on arbitrary assumptions and situations (e.g. the transmitted power, the area of the disk, the factor of propagation loss and so on), the achievable rate itself is not of interest. In order to compare the effects of node cooperation appropriately in various channel conditions, we use the same desired rate (5.0 b/s/Hz for about 15 dB average SNR) for all scenarios.

In addition, the percentage by which cooperative actions in a channel condition improves upon simple relays may not be constant with different node densities because the number of possible routes exponentially increases with the node density. We simulated low, middle and high density deployments (30, 40 and 50 nodes/disk respectively). Some fixed limited-peak powers which require at least 30, 40 and 50 nodes for the desired rate in a channel condition without node cooperation are used

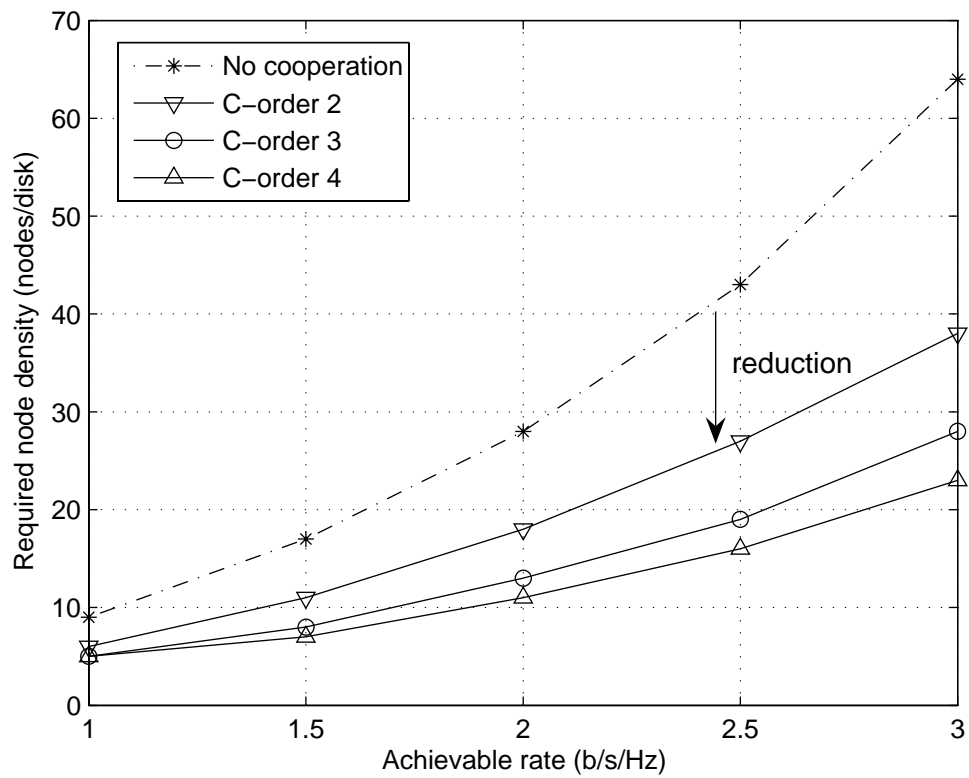


Figure 3.2: Required node density vs. achievable rate

for cooperative scenarios of the channel condition with low, middle and high density deployments respectively.

An optimistic upper bound on the reduction of node density will be found using the following assumptions: no shadowing, no interference among hops, perfect synchronization and perfect channel state information at the receiving nodes (CSIR).

It is assumed that the cooperative nodes are separated by a distance of more than several wavelengths of the carrier frequency for independence of paths. In simulations for all scenarios, we assume that the radius of a disk is 200m and the carrier frequency is 900MHz. We now describe several scenarios.

### 3.2.4 Channel Knowledge at the Transmitting Nodes

#### 3.2.4.1 Cooperative Transmission without CSIT

Without feed-back, the transmitting nodes do not have channel state information and it is reasonable to choose input signals to be spatially white [28], [30]–[32], i.e., the input covariance matrix in (3.7) without feedback is given by a diagonal matrix with the  $i$ th diagonal element  $P_{tx}^i/P_{lp}$  letting the index of the node corresponding to the  $i$ th diagonal element be  $i$ .

#### 3.2.4.2 Cooperative Transmission with Perfect CSIT

With feedback, the transmitting nodes can have channel state information and the achievable rate can be maximized using the water-filling algorithm [30]. The water-filling algorithm cannot be implemented under the limited-peak-power constraint per node, but the achievable rate can be improved using the optimized input covariance matrix,  $\mathbf{Q}_w$ , chosen so that the correlation between input signals maximizes the mutual information for a given channel. This is a constrained-nonlinear maximization

problem, i.e., for  $M_T \times M_R$  cooperative communication, it can be written as

$$\begin{aligned} & \text{maximize}_{\mathbf{Q}_w} && I(\mathbf{Q}_w) = \log_2 \det \left( \mathbf{I}_{M_R} + \frac{P_{lp}}{N_0} \mathbf{H} \mathbf{Q}_w \mathbf{H}^H \right) \\ & \text{subject to} && \begin{cases} \mathbf{Q}_w = E [\mathbf{A} \mathbf{s} \mathbf{s}^H \mathbf{A}^H] = \mathbf{A} \mathbf{A}^H \\ \|a_i\| \leq P_{tx}^i / P_{lp} \end{cases}, \end{aligned} \quad (3.12)$$

where  $\mathbf{A} \in \mathbb{C}^{M_T \times M_T}$  and  $a_i$  is the  $i$ th row of  $\mathbf{A}$ . The optimal  $\mathbf{Q}_w$  was searched using a non-linear program in *MATLAB* for each hop in the simulation.

## 3.2.5 Channel Models

### 3.2.5.1 Non-fading Gaussian Channel

$\mathbf{H}$  is assumed to be a deterministic channel matrix with real-valued elements determined by path gains. The element at the  $j$ th row and  $i$ th column of  $\mathbf{H}$  is [1]

$$h_{j,i} = \sqrt{g_{i,j}}. \quad (3.13)$$

The path gain between the  $i$ th transmitting node and  $j$ th receiving node,  $g_{i,j}$  is [1]

$$g_{i,j} \propto \left( \frac{d_{i,j}}{d_0} \right)^{-\alpha}, \quad (3.14)$$

where  $d_{i,j}$  is the distance between the  $i$ th transmitting node and  $j$ th receiving node,  $d_0$  is the reference distance ( $= 1m$ ) and  $\alpha$  is the factor of propagation loss. The factors 2, 3 and 4 are considered in this chapter. The achievable rate for each hop is obtained by (3.5).

### 3.2.5.2 Random Rayleigh Fading Channel

$\mathbf{H}$  is assumed to be a random channel matrix with complex-valued elements determined by path gains and Rayleigh-fading components. The element at the  $k$ th row and  $i$ th column is [1]

$$h_{k,i} = \sqrt{g_{i,k}} (x_{i,k} + jy_{i,k}), \quad (3.15)$$

where

$$x_{i,k} \sim \mathcal{N}(0, \sigma^2), \quad y_{i,k} \sim \mathcal{N}(0, \sigma^2), \quad (3.16)$$

$\sigma$  is the standard deviation of the Rayleigh fading component and the root-mean-squared (rms) value of the envelope of the received signal is normalized ( $2\sigma^2 = 1$ ). The achievable rate is obtained by (3.6) assuming that CSIT is available for slow-fading channels but not for fast-fading channels. We approximate the expectation value in (3.6) by averaging several thousand iterations.

### 3.2.5.3 Quasi-static Rayleigh Fading Channel

The channel is modeled to be fixed during a burst and randomly changes from burst to burst [31]. The achievable rate is calculated as if a randomly selected channel is unchanged during a burst. Thus the achievable rate is obtained by (3.5) with a realization of a random channel matrix  $\mathbf{H}$  which is selected by (3.15) and (3.16).

### 3.2.5.4 Ricean Fading Channel

The channel matrix  $\mathbf{H}$  is a complex-valued matrix determined by path gains and Ricean fading components. The element at the  $k$ th row and  $i$ th column of  $\mathbf{H}$  is same as (3.15) [1], [34], [35] where

$$x_{i,k} \sim \mathcal{N}(v \cos \theta, \sigma^2), \quad y_{i,k} \sim \mathcal{N}(v \sin \theta, \sigma^2), \quad (3.17)$$

$v$  is the Line-of-Sight (LOS) component,  $\sigma$  is the standard deviation of the fading component,  $\theta$  is any real number and the rms value is normalized ( $v^2 + 2\sigma^2 = 1$ ). We define the Ricean Factor ( $RF$ ) as  $RF = v^2/(v^2+2\sigma^2) = v^2$ . The Ricean fading channel reduces to a non-fading deterministic channel when  $RF = 100\%$  and a Rayleigh fading channel when  $RF = 0\%$ . CSIT is not considered. Both the random and quasi-static Ricean channels are simulated with a focus on the effect of fluctuation of path gains

in random fading channels and non-uniformity of path gains in quasi-static fading channels.

### 3.3 Simulation Results

The reduction in the node density required to guarantee a certain desired rate ( $5.0 \text{ b/s/Hz}$ ) with cooperation in various channel conditions for the middle density (40 nodes/disk without cooperation) is shown in Figs. 3.3 ~ 3.5.

We see that density decreases range from 25% to 80%, with greater benefits for lower  $\alpha$ , greater cooperation, and fading.

The cooperation has a slightly larger impact in the higher density examples

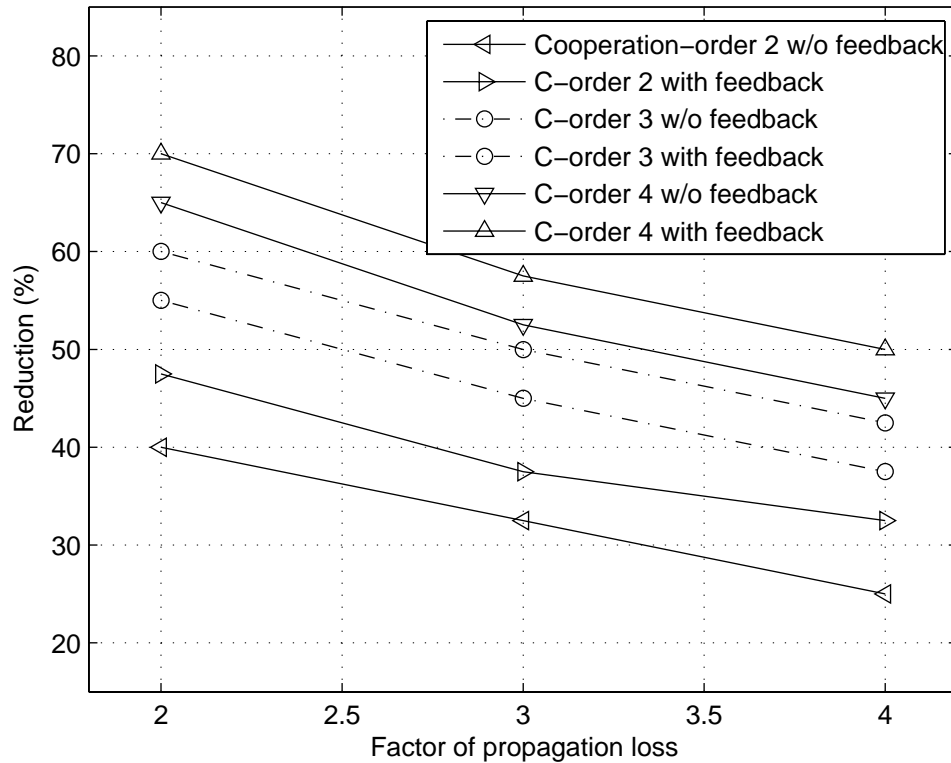


Figure 3.3: Reduction of node density in non-fading channels

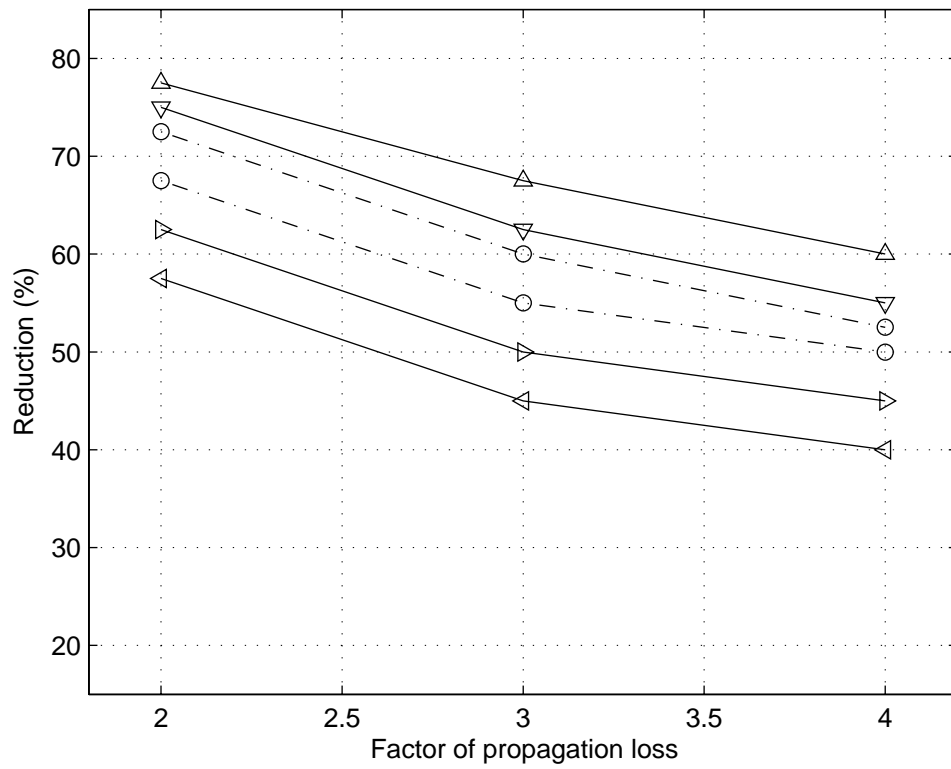


Figure 3.4: Reduction of node density in random Rayleigh fading channels

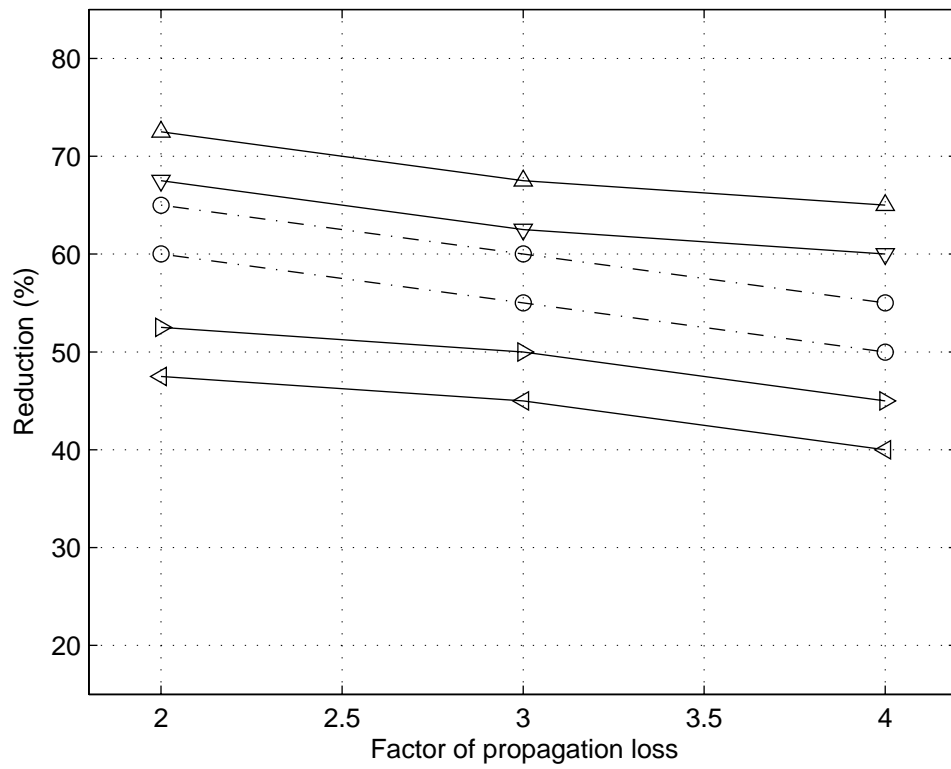


Figure 3.5: Reduction of node density in quasi-static Rayleigh fading channels

(0 ~ 5% more reduction in the high density than in the low density) due to the exponentially increased number of possible routes. For  $n$  nodes including a source and destination, the number of possible cooperation partners for cooperation-order  $m$  can be written as

$$\# \text{ cooperation partners} = \sum_{i=1}^m \binom{n-2}{i}. \quad (3.18)$$

Accordingly, the number of routes increases with cooperation. The number of routes without cooperation is

$$N_1 = 1 + (n-2) + (n-2)(n-3) + \cdots + (n-2)!. \quad (3.19)$$

For cooperation-order 2, it is given by

$$\begin{aligned} N_2 = & 1 + \left\{ (n-2) + \binom{n-2}{2} \right\} + \\ & \left[ (n-2) \left\{ (n-3) + \binom{n-3}{2} \right\} + \right. \\ & \left. \binom{n-2}{2} \left\{ (n-4) + \binom{n-4}{2} \right\} \right] + \cdots. \end{aligned} \quad (3.20)$$

The first term of the right side in (3.19) and (3.20) is the number of one-hop routes (i.e., 1), the second term is the number of two-hop routes and so on. Some examples of the increase of possible routes with node density and cooperation are shown in Table 3.1.

The effect decreases as the propagation factor  $\alpha$  increases because cooperation's effect on the capacity of (3.5) and (3.6) is smaller and it is more difficult to overcome

Table 3.1: Examples for the number of possible routes

<b># Nodes</b>	<b>Cooperation order 1</b>	<b>2</b>	<b>3</b>	<b>4</b>
10	109,601	801,705	1,049,281	1,087,081
20	1.7403e+016	2.8802e+018	5.9931e+018	6.6695e+018

the geographic spread with a smaller node density in worse propagation environments. Defining the coverage of a node as the maximum distance which the node can communicate while meeting a QoS threshold, assume that the coverages of each node are  $c_{nc}$  and  $c_c$  without and with cooperation respectively ( $c_{nc} \leq c_c$ ) for a propagation factor  $\alpha_1$ . If the required node densities are  $d_{nc}(\alpha_1)$  without cooperation and  $d_c(\alpha_1)$  with cooperation, then the ratio is

$$\frac{d_c(\alpha_1)}{d_{nc}(\alpha_1)} = \left( \frac{c_{nc}}{c_c} \right)^2. \quad (3.21)$$

The coverage  $c_{nc}$  and  $c_c$  are changed to  $c_{nc}^{\alpha_1/\alpha_2}$  and  $c_c^{\alpha_1/\alpha_2}$  respectively for another propagation factor  $\alpha_2$ . Then the ratio of the required node density is

$$\frac{d_c(\alpha_2)}{d_{nc}(\alpha_2)} = \left( \frac{c_{nc}}{c_c} \right)^{2\alpha_1/\alpha_2} \quad (3.22)$$

and it is derived that

$$\frac{d_c(\alpha_1)}{d_{nc}(\alpha_1)} \leq \frac{d_c(\alpha_2)}{d_{nc}(\alpha_2)} \quad \text{for } \alpha_2 \geq \alpha_1. \quad (3.23)$$

It is simply proved in (3.23) that a larger propagation factor yields less effect on the reduction of node density with cooperation. Cooperation-order 2 provides only modest reductions in node density even under our idealized assumptions for propagation factor 4, casting doubt on its utility for large propagation losses.

CSIT gives additional improvement of only 5 ~ 10% or less due to the limited-peak-power constraint per node under which the water-filling algorithm [30] cannot be implemented. Cooperation results in significant gains in many scenarios. Simulation results show greater gains of cooperation in both the random and quasi-static Rayleigh fading channels than in non-fading channels.

### 3.3.1 Path Diversity

One interesting result is that the effects of cooperation in *random* Rayleigh fading channels are larger than in non-fading channels (Figs. 3.3 and 3.4). We can see about

10 ~ 15% more reduction in random Rayleigh fading channels than in non-fading channels for all propagation factors.

Fading components produce a degradation of the capacity in SISO channels but a benefit in the capacity for MIMO channels [34]. Therefore, the improvement in the MIMO capacity increases as the fading component increases (or  $RF$  decreases) in the Ricean fading channel [34], [35]. Simulations in random Ricean fading channels show the relation between the fading component and the effect of cooperation (see Figs. 3.6 and 3.7). It is not surprising that the node densities with high-ordered cooperation do not decrease as  $RF$  decreases because lower-ordered cooperation always contributes considerably for the scenarios with higher-ordered cooperation.

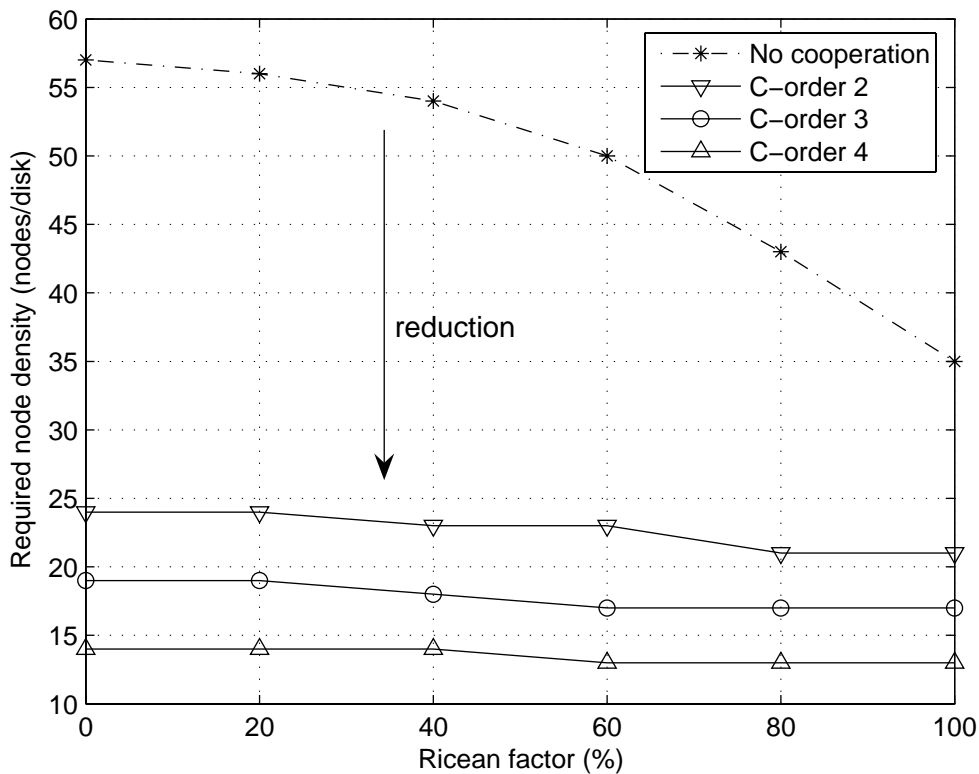


Figure 3.6: Required node density in random Ricean channels

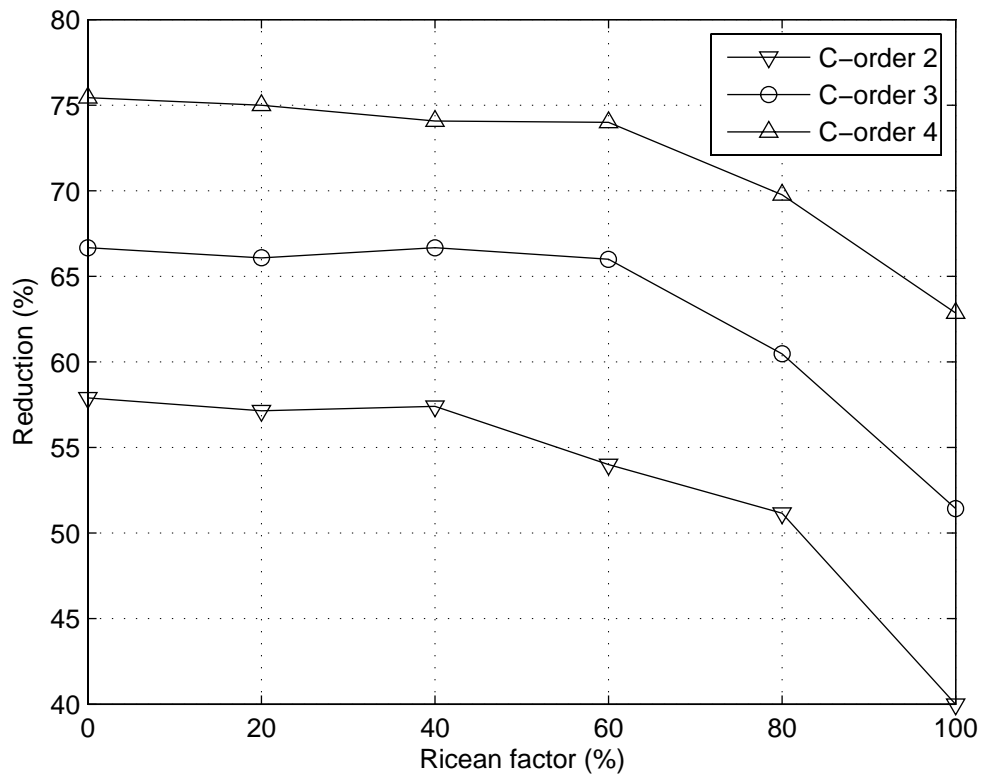


Figure 3.7: Reduction of node density in random Ricean channels

Since cooperation yields a larger reduction in node density as the fading component increases as Fig. 3.7, it is clear that the effects of cooperation in random Rayleigh fading channels are greater than in non-fading channels as Figs. 3.3 and 3.4.

### 3.3.2 Non-uniformity

Another interesting result is that the effects of cooperation in *quasi-static* Rayleigh fading channels are a little larger than in non-fading channels and smaller than in random Rayleigh fading channels for  $\alpha = 2$ , and become closer to the random Rayleigh fading channels for larger propagation factors. The quasi-static Rayleigh fading channels have about 5, 10, and 15% more reduction than non-fading channels for the propagation factors 2, 3, and 4 respectively (Figs. 3.3 and 3.5).

In the quasi-static fading channels, it is assumed that the path gain changes randomly but it lasts over a burst [31] even though the average behaviors converge to the random fading channels. This makes the space with small propagation factors non-uniform in the sense of path gain (i.e., larger variance), in contrast to non- or random-fading channels and this non-uniformity increases the probability of there existing at least one good route. But the non-uniformity from the quasi-static fading vanishes with large propagation factors and the path gains in the quasi-static Rayleigh fading channels becomes more uniform than in other channels for  $\alpha = 4$ .

The expected values of the best several path gains for each node in non-fading and quasi-static Rayleigh fading channels can be computed by order statistics [36]. The probability density function (pdf) of the  $k$ th statistic out of  $n$  independently drawn values of a random variable  $Z$  is given by [36]

$$f_{Z_{(n,k)}}(z) = n \binom{n-1}{k-1} F_Z(z)^{k-1} (1 - F_Z(z))^{n-k} f_Z(z), \quad (3.24)$$

where  $F_Z(\cdot)$  is the cumulative distribution function (cdf) and  $f_Z(\cdot)$  is the pdf of  $Z$ .

Thus the expected value of the  $k$ th ordered  $Z$  out of  $n$  draws is given by

$$E [Z_{(n,k)}] = \int z f_{Z_{(n,k)}}(z) dz. \quad (3.25)$$

For example, the expected value of the maximum or minimum out of  $n$  can be obtained by assigning  $k = n$  or  $k = 1$  respectively.

It is assumed that a source is located at the center of a disk with a radius  $r$ ,  $n$  other nodes are deployed randomly in the disk and away from the source by at least a reference distance  $d_0$ . The cdf and pdf of the path gains from the source and other nodes in non-fading channels are derived as

$$F_X(x) = 1 - \frac{x^{-2/\alpha} - d_0^2}{r^2 - d_0^2}, \quad \text{for } r^{-\alpha} \leq x \leq d_0^{-\alpha}, \quad (3.26)$$

$$f_X(x) = \frac{2x^{(-2/\alpha)-1}}{\alpha (r^2 - d_0^2)}, \quad \text{for } r^{-\alpha} \leq x \leq d_0^{-\alpha}, \quad (3.27)$$

where  $X = D^{-\alpha}$  and  $D$  is the distance between the source and another node. The cdf of the path gains in quasi-static Rayleigh channels is expressed as

$$F_Y(y) = \int_{d_0}^r F_T(\sqrt{ys^\alpha}) f_D(s) ds, \quad \text{for } y \geq 0, \quad (3.28)$$

where  $Y = D^{-\alpha}T^2$ ,  $T$  is the Rayleigh random variable,  $F_T(\cdot)$  is the cdf of  $T$  and  $f_D(\cdot)$  is the pdf of  $D$ . The cdf and pdf of  $Y$  can be easily derived as closed forms when  $\alpha = 2$ ,

$$F_Y(y) = 1 + \frac{e^{-yr^2} - e^{-yd_0^2}}{y (r^2 - d_0^2)}, \quad \text{for } y \geq 0, \quad (3.29)$$

$$f_Y(y) = \frac{d_0^2 e^{-yd_0^2} - r^2 e^{-yr^2}}{y (r^2 - d_0^2)} + \frac{e^{-yd_0^2} - e^{-yr^2}}{y^2 (r^2 - d_0^2)}, \quad \text{for } y \geq 0. \quad (3.30)$$

The expected values of  $X_{(n,n)}$  and  $Y_{(n,n)}$  which are the highest-ordered path gains, and the several high-ordered path gains out of  $n$  paths in non- and quasi-static Rayleigh fading channels are compared in Figs. 3.8 and 3.9 using (3.24)–(3.30). Only a few path gains (about 5 ~ 6) are magnified and higher-ordered path gains are magnified more.

Since the non-uniformity statistically magnifies the highest ordered path gain and does not alter the others much, it mainly helps in non-cooperative scenarios to reduce node densities and decreases the effect of cooperation. The effect of the quasi-static fading

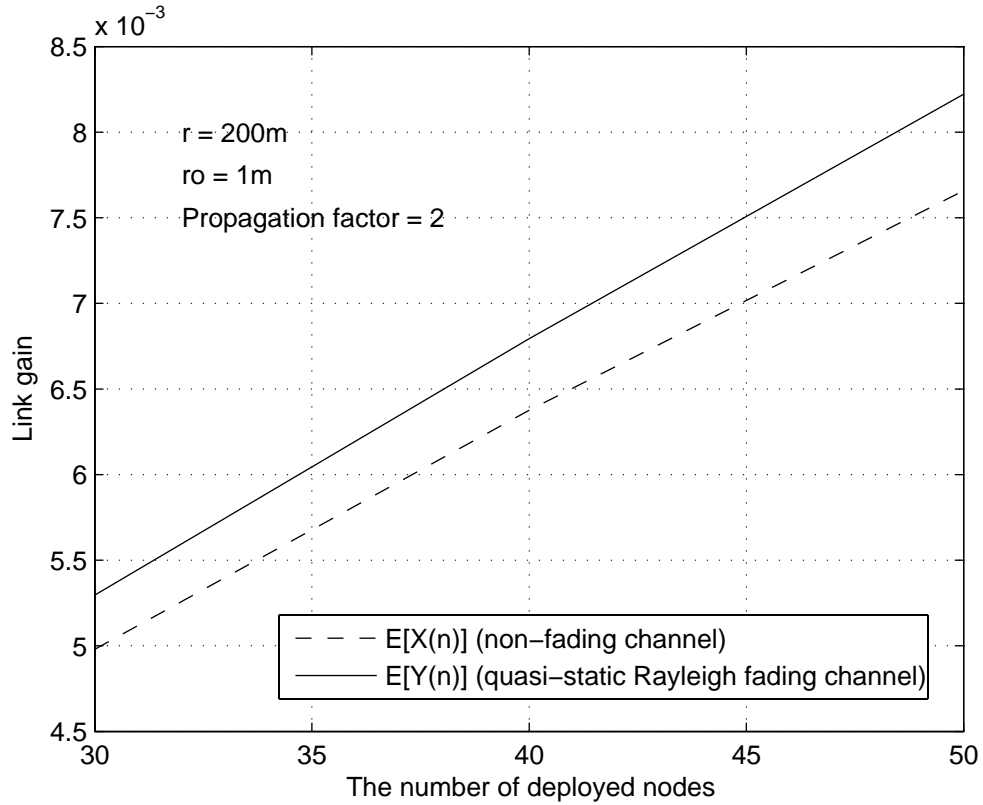


Figure 3.8: The expected largest path gain with  $\alpha = 2$

components in Ricean channels with  $\alpha = 2$  is shown in Figs. 3.10 and 3.11. Since the non-uniformity makes a remarkable contribution to non-cooperative scenarios while the path diversity is still a benefit for cooperative ones in fading channels, the effect of cooperation in quasi-static Rayleigh channels are less than in random Rayleigh channels for  $\alpha = 2$  and become similar for  $\alpha = 3, 4$ .

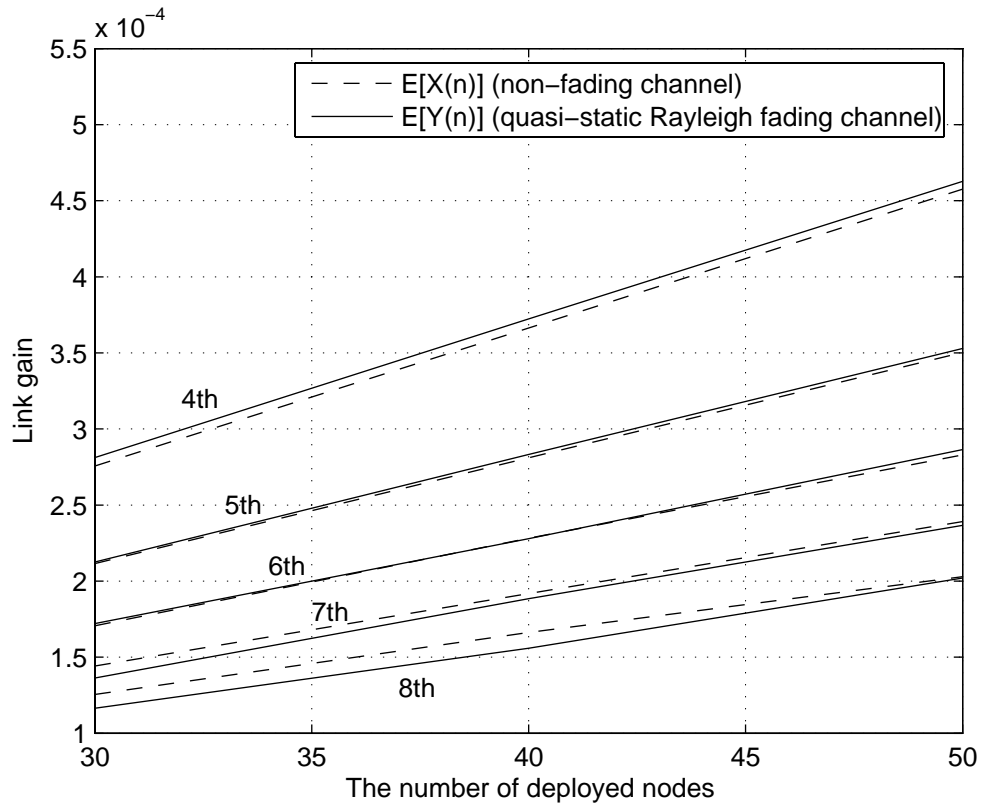


Figure 3.9: The expected values of the largest several path gains with  $\alpha = 2$

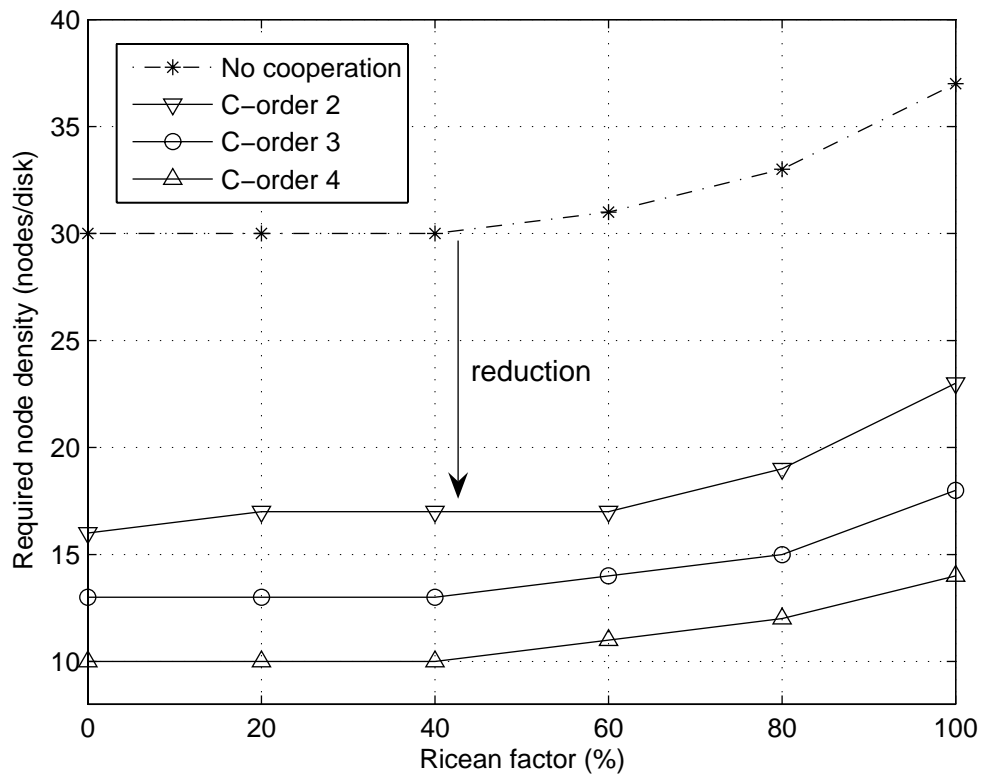


Figure 3.10: Required node density in quasi-static Ricean channels with  $\alpha = 2$

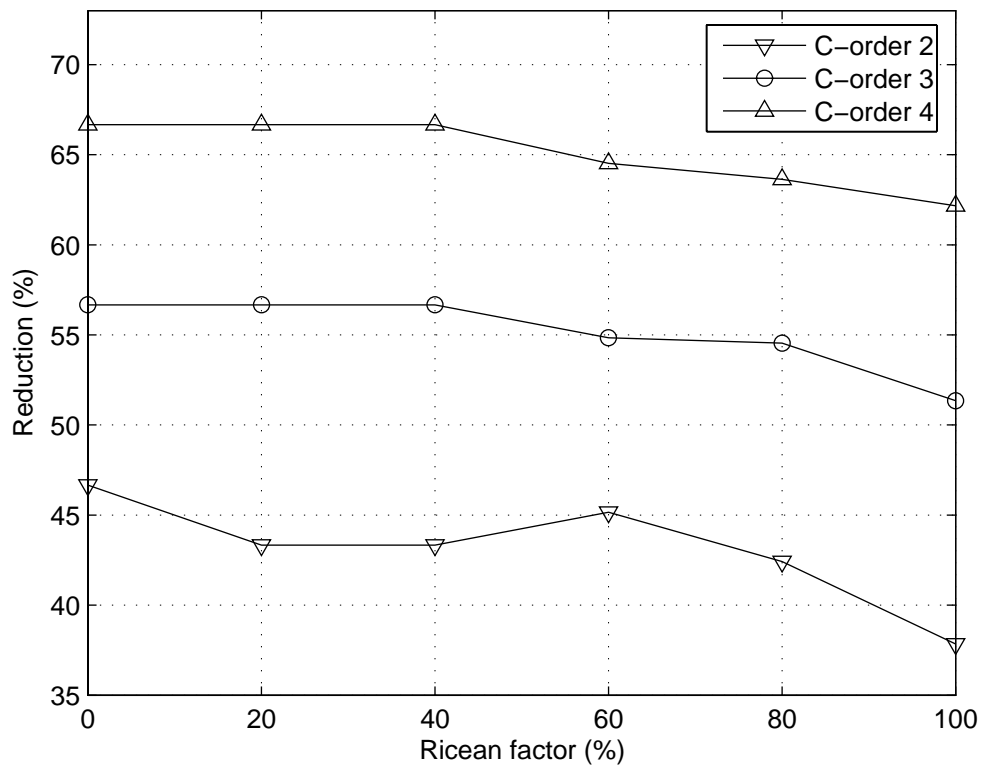


Figure 3.11: Reduction of node density in quasi-static Ricean channels with  $\alpha = 2$

## 3.4 Conclusion

For the scenarios considered, node density reductions ranged from 25% to 80% with cooperation on individual hops, assuming synchronization is free, channel state information is available in the receiver, and optimal routes could be found in a timely manner. This gain is derived from the benefit of the path diversity and disturbed by the non-uniformity. The path diversity that improves capacity in each hop is the main benefit for all scenarios, especially for random fading channels. The non-uniformity in the sense of path gain gives the magnification of the best few paths for each node and increases the probability of there existing at least one good route in quasi-static fading channels. This results in better routing with the non-cooperative communication. At the low end of the potential gains, implementation losses and the considerable increase in complexity argue that simple relay strategies are probably sufficient. At the higher end, the research suggests there is value in pursuing practical algorithms to effect the cooperation.

# Chapter 4

## Cooperative Power Control with Fast Convergence

### 4.1 Introduction

Power control plays a critical role improving the performance of communication systems. Effective transmitter power control increases the overall network capacity in many situations. More transmitters can communicate with their intended receivers simultaneously in a network and their batteries can live longer since effective power control keeps transmitters from spending redundant power while guaranteeing required link qualities if they are feasible in the network.

Zander [37], and Grandhi *et al.* [38] studied centralized power control algorithms. They solved an eigenvalue problem for the optimal transmitting powers. The optimal power vector was found as an eigenvector associated with a positive eigenvalue of a scaled cross-link gain matrix.

Distributed asynchronous power control algorithms were proposed by Foschini and Miljanic [39], and Mitra [40]. Due to the computational complexity and difficulty of

gathering overall information of a network in centralized algorithms, the distributed algorithms are very attractive. Many interesting distributed power control algorithms with realistic constraints have been proposed. Grandhi *et al.* [41] considered an upper limit of transmitting power, and Bambos, Chen and Pottie [42] proposed a distributed algorithm protecting active links with realistic call arrivals.

Centralized algorithms require added infrastructure, and suffer from latency and network vulnerability [39]. Distributed algorithms are inescapably iterative and the convergence speed is one of the most important criteria along with the stability. The question thus naturally arises as to which algorithm improves the network capacity more. The answer must be dependent on the capability of the central infrastructure of a network system, and the relative latencies of centralized control and distributed iterations. If a tradeoff between the latencies from the centralization and distributed iterations is investigated, then the minimum overall latency can be obtained and it will be the answer to improve the network capacity most.

In this chapter, we propose a cooperative power control algorithm and analyze its convergence. Only a single group of some links may be capable of cooperating, or multiple groups of links may be capable of cooperating independently. The cooperative groups share information on transmitting powers, locally measured interference, and cross-link gains. In real wireless network systems, it is not always possible to figure out the complete cross-link gains rather than the powers and interferences especially in ad-hoc network systems. The cooperative power control algorithm proposed here works well for a generalized scenario, with locally-cooperating multiple independent groups sharing incomplete information of cross-link gains. The enhancement on the convergence speed of the cooperative algorithm is proved with eigenvalue analysis.

The rest of the chapter is organized as follows. In Section 4.2, we describe the system model and the distributed power control algorithm [39]. The cooperative

power control algorithm and its convergence are investigated in Section 4.3. In Section 4.4, simulation results are shown, and we conclude in Section 4.5.

## 4.2 System Model

We consider the wireless network to be a collection of radio links. The links correspond to transmissions between transmitters and their intended receivers. These can be transmissions between mobiles and a base station (BS) in cellular networks, or single-hop transmissions between transmitting-receiving nodes pairs in ad-hoc networks.

The quality of each link can be determined by the signal-to-interference ratio (SIR) at its receiver. We denote the SIR of the  $i$ th link among all  $M \in \mathbb{Z}_+$  links as

$$R_i = \frac{G_{ii}P_i}{\sum_{j \neq i} G_{ij}P_j + \eta_i}, \quad i, j \in \{1, \dots, M\}, \quad (4.1)$$

where  $G_{ij} \geq 0$  is the link gain from the transmitter of the  $j$ th link to the receiver of the  $i$ th link (not necessarily strictly positive except for  $i = j$ ),  $P_i$  is the transmitting power of the  $i$ th link, and  $\eta_i$  is the thermal noise power at the receiver of the  $i$ th link.

With minimum SIR requirements  $\gamma_i > 0$  of the  $i$ th link for a minimum QoS that the link must support, the well-known matrix form is given by [39], [42]

$$(\mathbf{I} - \mathbf{F}) \mathbf{P} \geq \mathbf{u} \quad \text{and} \quad \mathbf{P} > \mathbf{0}, \quad (4.2)$$

where  $\mathbf{P} = (P_1, \dots, P_M)^T$  is the vector of transmitting powers, the appropriately scaled matrix  $\mathbf{F}$  of cross-link gains is given by

$$\mathbf{F}^{(i,j)} = \begin{cases} 0, & i = j \\ \frac{\gamma_i G_{ij}}{G_{ii}}, & i \neq j \end{cases}, \quad i, j \in \{1, \dots, M\}, \quad (4.3)$$

the appropriately scaled vector of thermal noise powers is given by

$$\mathbf{u} = \left( \frac{\gamma_1 \eta_1}{G_{11}}, \dots, \frac{\gamma_M \eta_M}{G_{MM}} \right)^T, \quad (4.4)$$

and the inequality constraint is component-wise in this chapter.

The non-negative matrix  $\mathbf{F}$  is not necessarily but reasonably assumed *irreducible* since any isolated groups of links that do not interact with all other links in the network do not need to be considered (if there are, the isolated groups can be handled as independent networks) [42]. By the irreducibility and non-negativity, the Perron-Frobenius theorem and some related theorems [43] are applicable.

Let  $\widehat{\lambda}(\mathbf{F})$  the maximum modulus eigenvalue of  $\mathbf{F}$ , defined as [39]

$$\widehat{\lambda}(\mathbf{F}) = \min_{x \in X_+} \left[ \min_{\mu} (\text{real } \mu \text{ such that } \mathbf{F}x - \mu x \leq 0) \right], \quad (4.5)$$

where  $X_+$  is the set of all  $M$  dimensional vectors,  $x$ , other than the zero vector, that satisfy  $x > 0$ . If  $\widehat{\lambda}(\mathbf{F}) < 1$ , then

$$\mathbf{P}^* = (\mathbf{I} - \mathbf{F})^{-1} \mathbf{u} \quad (4.6)$$

is the Pareto optimal solution of (4.2), and it is the best target of most power control algorithms because if any other solution  $\mathbf{P}$  of (4.2) exists, then  $\mathbf{P} \geq \mathbf{P}^*$ .

## 4.2.1 Distributed Power Control

The distributed power control algorithm based on local SIR (or local interference) proposed by Foschini and Miljanic [39] is simplified as [42]

$$P_i(k+1) = \frac{\gamma_i}{R_i(k)} P_i(k) = \frac{\gamma_i}{G_{ii}} I_i(k), \quad i \in \{1, \dots, M\}, \quad (4.7)$$

where the time index  $k = 1, 2, \dots$ , and  $I_i(k)$  is the interference measured by the receiver of the  $i$ th link. This algorithm can be represented by matrix forms,

$$\mathbf{P}(k+1) = \mathbf{F}\mathbf{P}(k) + \mathbf{u} \quad \text{for } \beta = 1, \quad (4.8)$$

where the proportionality constant  $\beta$  (need to be unity for universal convergence [39]).

If  $\widehat{\lambda}(\mathbf{F}) < 1$ , then the iteration of (4.8) converges to  $\mathbf{P}^*$  in (4.6),

$$\lim_{k \rightarrow \infty} \mathbf{P}(k) = \lim_{k \rightarrow \infty} \mathbf{F}^k \mathbf{P}(0) + \lim_{k \rightarrow \infty} \sum_{i=0}^{k-1} \mathbf{F}^i \mathbf{u} = (\mathbf{I} - \mathbf{F})^{-1} \mathbf{u} = \mathbf{P}^*. \quad (4.9)$$

Each link increases its power when its current SIR is below its target value  $\gamma_i$ , and decreases it otherwise [42]. We recognize from (4.7) that each link tries to achieve its target SIR value autonomously assuming its interference amount at the current time index will not be changed at the next time index. This assumption guarantees the convergence of (4.8) when  $\widehat{\lambda}(\mathbf{F}) < 1$  and it is a reasonable assumption without any information regarding other links. But since  $\mathbf{F}$  is irreducible, the power update of even one link causes a change of interference to all others, and eventually turns into a change of interference to itself that must be overcome to achieve its target SIR value. This *ping-pong* effect is the reason why distributed power control algorithms converge slowly, especially in the strongly interference-coupled network. It is unavoidable with their distributed features.

### 4.3 Cooperative Power Control

As shown so far, the *ping-pong* effect and the assumption of unchanged future interference state slow down the convergence speed even though they are inevitable without any information concerning other links. If some links cooperate (or are the control of a local manager), they can predict the variation of future interference state more reliably through estimating the interactions among the cooperative links. We will show that this brings a substantial improvement in the convergence speed.

#### 4.3.1 Cooperative Power Control Algorithm

Let the  $n$  cooperative links with the index  $1, 2, \dots, n$  ( $n \leq M$ ) share information concerning transmitting powers and locally measured interference, and some identified cross-link gains among them (not necessarily all  $n^2 - n$  values like the cooperative group 2 in Fig. 4.1). Then they can figure out what amount of interference is caused by

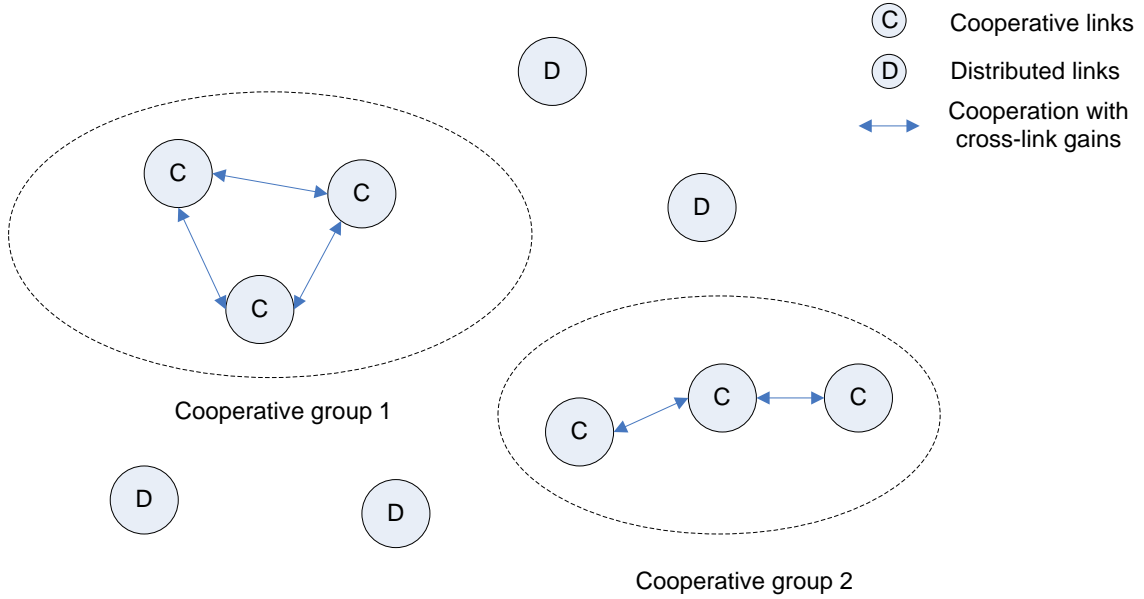


Figure 4.1: Cooperative Groups and Distributed (Non-cooperative) links (cells or P2P pairs)

the cooperative links whose cross-link gains are identified. We propose a cooperative power control algorithm which estimates the interactions among the cooperative links using the centralized algorithm of (4.6), assuming the unidentified interference will be handled using the idea of the distributed algorithm in (4.7). The unidentified interference at the receiver of the  $i$ th link at time  $k$  is

$$\tilde{I}_i(k) = I_i(k) - \hat{I}_i(k), \quad i \in \{1, \dots, n\} . \quad (4.10)$$

The identified interference  $\hat{I}_i(k)$  is written as

$$\hat{I}_i(k) = \sum_{(j \rightarrow i) \in C_p} G_{ij} P_j(k), \quad i, j \in \{1, \dots, n\} , \quad (4.11)$$

where  $C_p$  is the index pairs set of identified cross-link gains among the cooperative links. The scaled noise power vector of (4.4) is replaced with the unidentified

interference vector,

$$\tilde{\mathbf{u}}_c(k) = \left( \frac{\gamma_1 \tilde{I}_1(k)}{G_{11}}, \dots, \frac{\gamma_n \tilde{I}_n(k)}{G_{nn}} \right)^T. \quad (4.12)$$

The identified cross-links gains which the cooperative links group shares are represented as an  $n \times n$  matrix (called a “group cooperation matrix” in this chapter),

$$\mathbf{F}_{c(i,j)} = \begin{cases} 0, & i = j \\ \frac{\gamma_i G_{ij}}{G_{ii}}, & i \neq j, (j \rightarrow i) \in Cp \end{cases}, \quad i, j \in \{1, \dots, n\}. \quad (4.13)$$

**Theorem 1.** When the feasible power vector  $\mathbf{P}^* = (\mathbf{I} - \mathbf{F})^{-1} \mathbf{u}$  exists,  $\mathbf{I}_n - \mathbf{F}_c$  is invertible for a group cooperation matrix  $\mathbf{F}_c$ .

**Proof:** see Appendix A.1.

By Theorem 1, the update of power vector of the cooperative links is suggested as

$$\mathbf{P}_c(k+1) = (\mathbf{I}_n - \mathbf{F}_c)^{-1} \tilde{\mathbf{u}}_c(k), \quad (4.14)$$

where  $\mathbf{P}_c = (P_1, \dots, P_n)^T$  and  $\mathbf{I}_n$  is the  $n \times n$  identity matrix. The  $M - n$  non-cooperative links follow the distributed algorithm of (4.7) and (4.8).

### 4.3.2 Convergence

The unidentified interference vector in (4.12) is represented in matrix form as

$$\tilde{\mathbf{u}}_c(k) = \mathbf{I}_{n0} [(\mathbf{F} - \mathbf{F}_{c0}) \mathbf{P}(k) + \mathbf{u}], \quad (4.15)$$

where  $\mathbf{I}_{n0} = \begin{pmatrix} \mathbf{I}_n & \mathbf{0}_{n \times (M-n)} \end{pmatrix}$  and  $\mathbf{F}_{c0} = \begin{pmatrix} \mathbf{F}_c & \mathbf{0}_{n \times (M-n)} \\ \mathbf{0}_{(M-n) \times n} & \mathbf{0}_{(M-n) \times (M-n)} \end{pmatrix}$  have been augmented using an  $a \times b$  zero matrix  $\mathbf{0}_{a \times b}$  for  $a, b \in \mathbb{Z}_+$ . The update of power vector (4.14) is written as

$$\mathbf{P}_c(k+1) = (\mathbf{I}_n - \mathbf{F}_c)^{-1} \mathbf{I}_{n0} [(\mathbf{F} - \mathbf{F}_{c0}) \mathbf{P}(k) + \mathbf{u}]. \quad (4.16)$$

Therefore the whole power vector including the non-cooperative links is derived as

$$\mathbf{P}(k+1) = (\mathbf{I} - \mathbf{F}_{c_0})^{-1} [(\mathbf{F} - \mathbf{F}_{c_0}) \mathbf{P}(k) + \mathbf{u}]. \quad (4.17)$$

More generally for independently cooperating  $m$  groups  $c_1, \dots, c_m$  with an index pairs set of identified cross-link gains  $Cp$ , the group cooperation matrices  $\mathbf{F}_{c_l}$  are written without loss of generality as

$$\mathbf{F}_{c_l(\hat{i}, \hat{j})} = \begin{cases} 0, & \hat{i} = \hat{j} \\ \frac{\gamma_i G_{ij}}{G_{ii}}, & \hat{i} \neq \hat{j}, (j \rightarrow i) \in Cp \end{cases}, \quad (4.18)$$

for  $\hat{i}, \hat{j} = 1, \dots, M_{c_l}$ ,  $i = \sum_{u=1}^{l-1} M_{c_u} + \hat{i}$ ,  $j = \sum_{u=1}^{l-1} M_{c_u} + \hat{j}$ ,  $l = 1, \dots, m$ , where  $M_{c_l}$  is the number of links in the group  $c_l$ . The associated “network cooperation matrix”  $\mathbf{C}$  and  $(\mathbf{I} - \mathbf{C})^{-1}$  are given by

$$\mathbf{C} = \begin{pmatrix} \mathbf{F}_{c_1} & \mathbf{0} & \mathbf{0} & \mathbf{0} \\ \mathbf{0} & \ddots & \mathbf{0} & \mathbf{0} \\ \mathbf{0} & \mathbf{0} & \mathbf{F}_{c_m} & \mathbf{0} \\ \mathbf{0} & \mathbf{0} & \mathbf{0} & \mathbf{0} \end{pmatrix} \quad \text{and} \quad (4.19)$$

$$(\mathbf{I} - \mathbf{C})^{-1} = \begin{pmatrix} (\mathbf{I}_{M_{c_1}} - \mathbf{F}_{c_1})^{-1} & \mathbf{0} & \mathbf{0} & \mathbf{0} \\ \mathbf{0} & \ddots & \mathbf{0} & \mathbf{0} \\ \mathbf{0} & \mathbf{0} & (\mathbf{I}_{M_{c_m}} - \mathbf{F}_{c_m})^{-1} & \mathbf{0} \\ \mathbf{0} & \mathbf{0} & \mathbf{0} & \mathbf{I}_{M_d} \end{pmatrix}, \quad (4.20)$$

where  $M_d$  is the number of the non-cooperative links ( $M = M_{c_1} + \dots + M_{c_m} + M_d$ ).

Then the update of power vector is derived as

$$\mathbf{P}(k+1) = (\mathbf{I} - \mathbf{C})^{-1} [(\mathbf{F} - \mathbf{C}) \mathbf{P}(k) + \mathbf{u}] = [\mathbf{I} - (\mathbf{I} - \mathbf{C})^{-1} (\mathbf{I} - \mathbf{F})] \mathbf{P}(k) + (\mathbf{I} - \mathbf{C})^{-1} \mathbf{u}. \quad (4.21)$$

This power update is identical to the distributed power control algorithm of (4.8) with  $\mathbf{C} = \mathbf{0}$  (no cooperation) and it evolves to the centralized equation of (4.6) with  $\mathbf{C} = \mathbf{F}$  (complete cooperation of all links).

**Theorem 2.** When the feasible power vector  $\mathbf{P}^* = (\mathbf{I} - \mathbf{F})^{-1} \mathbf{u}$  exists, the matrix updating power vector in (4.21) has the maximum modulus eigenvalue less than unity, i.e.,  $\hat{\lambda}(\mathbf{I} - (\mathbf{I} - \mathbf{C})^{-1}(\mathbf{I} - \mathbf{F})) < 1$ .

**Proof:** see Appendix A.2.

By Theorem 2, the cooperative power control algorithm (4.21) converges to the Pareto optimal solution (4.6),

$$\lim_{k \rightarrow \infty} \mathbf{P}(k) = [(\mathbf{I} - \mathbf{C})^{-1}(\mathbf{I} - \mathbf{F})]^{-1}(\mathbf{I} - \mathbf{C})^{-1} \mathbf{u} = (\mathbf{I} - \mathbf{F})^{-1} \mathbf{u} = \mathbf{P}^*. \quad (4.22)$$

### 4.3.3 Convergence Speed

Let  $Cp$  be an index pairs set of identified cross-link gains for  $m$  cooperative groups, and  $Cp^+$  another set having one or more index pairs of identified cross-link gains than  $Cp$  does with  $m^+$  cooperative groups. Let  $\mathbf{C}$ ,  $\mathbf{F}_{c_u}$  for  $u = 1, \dots, m$  and  $\mathbf{C}^+$ ,  $\mathbf{F}_{c_l^+}$  for  $l = 1, \dots, m^+$  be the associated network cooperation matrices and group cooperation matrices with  $Cp$  and  $Cp^+$  respectively. The number of cooperative groups of  $Cp^+$ ,  $m^+$  can be greater or less than the number of cooperative groups of  $Cp$ ,  $m$  (not necessarily  $m^+ > m$ ). If some non-cooperative links in  $Cp$  construct new cooperative groups with the additional identified cross-link gains with  $Cp^+$ , then  $m^+ > m$ . If some cooperative groups in  $Cp$  have more identified cross-link gains for their groups only with  $Cp^+$  and non-cooperative links do not have any changes, then  $m^+ = m$ . If some cooperative groups in  $Cp^+$  merge into one group with the additional identified cross-link gains with  $Cp^+$ , then  $m^+ < m$ .

**Theorem 3.** If the cooperative algorithm (4.21) with a network cooperation matrix  $\mathbf{C}$  converges to the Pareto optimal solution, then the cooperative algorithm with

$\mathbf{C}^+$  converges faster than with  $\mathbf{C}$  where the network cooperation matrix  $\mathbf{C}^+$  has additional cross-link gains compared to  $\mathbf{C}$ . That is, if  $\hat{\lambda}(\mathbf{I} - (\mathbf{I} - \mathbf{C})^{-1}(\mathbf{I} - \mathbf{F})) < 1$  and  $\mathbf{C}^+ \geq \mathbf{C}$  ( $\mathbf{C}^+ \neq \mathbf{C}$ ), then  $\hat{\lambda}(\mathbf{I} - (\mathbf{I} - \mathbf{C}^+)^{-1}(\mathbf{I} - \mathbf{F})) < \hat{\lambda}(\mathbf{I} - (\mathbf{I} - \mathbf{C})^{-1}(\mathbf{I} - \mathbf{F}))$ .

**Proof:** see Appendix A.3.

## 4.4 Simulation Results

We investigate the convergence speed of the cooperative power control in a cellular network system. We consider 10 randomly placed users in each of 61 hexagonal cells with their BSs at the centers of cells. The distance between the closest BSs is 1km. The link gains are modeled with the path loss exponent 4, the shadowing with a mean of 0dB and a standard deviation of 8dB, and the receiver noise level of -174dBm [1]. The users are assumed immobile during the power control iterations. The minimum SIR requirement  $\gamma$  for each user is chosen uniformly (for convenience) as 10dB. 10,000 independent feasible experiments are performed and averaged for each result.

For each experiment,  $\binom{M}{2} \times 2 = M^2 - M = 90$  levels of cooperation are compared with the distributed algorithm. We first consider a realistic cooperation scenario (scenario 1) in which cross-links expected to be most strongly coupled are considered to cooperate first. Two geometrically closest cells are selected, and they share one of the cross-link gains between them as the first level and the other one as the second level. The next two closest cells (one of the two cells selected in the previous levels can be selected again) are selected for the next two levels. The new selected two links (cells) may be already in a cooperative group, sharing the power and interference information only before the sharing of the cross-link gains. Otherwise one of them may join a cooperative group in which another has already joined, or they may construct a new cooperative group. For comparison, two more scenarios are considered. Scenario 2 is a cooperation scenario with the reverse order of scenario 1. In scenario 3, information

on randomly selected links is shared.

The initial powers for each experiment are randomly chosen from  $[0, 1]$  and the iterative algorithms are considered to converge to their optimal solutions at the  $k$ th iteration where  $|R_i(k) - \gamma_i| \leq \epsilon_i$  for  $i \in \{1, \dots, M\}$  and  $\epsilon_i = 0.01 \cdot \gamma_i$  (1% tolerance). The four cooperation levels (including the distributed algorithm) are normalized as the cooperation amounts with the range of  $[0, 1]$  defined as the number of identified/shared cross-link gains divided by  $M^2 - M$ .

The number of iterations and the maximum modulus eigenvalue are shown in Figs. 4.2 and 4.3. The convergence time and the maximum modulus eigenvalue are decreasing for all scenarios as the cooperation scope increases. As expected, it is shown in Figs. 4.2 and 4.3 that the cooperation between more strongly coupled cross-links (cells) makes a greater contribution to the convergence speed. Thus scenario 1 is both a realistic and good strategy for cooperative power control algorithms. The number of iterations is reduced by half with only 10% of interferers cooperating, and by a fourth with 25% cooperation in the scenario 1.

If the latency from the centralization is given, then the optimal cooperation level can be found. For example, for a simple linear function as the centralization latency, then the overall latency can be computed as shown in Fig. 4.4.

## 4.5 Conclusion

In this chapter, we have presented a cooperative power control algorithm and proved that the cooperation enhances the convergence speed. The cooperation scheme requires sharing information regarding power, interference, and cross-link gains. The cooperative links predict the future interference state as reliably as possible with the shared information. This brings a significant improvement in the convergence speed. In practice, it is difficult to identify the cross-link gains. It is proved by the eigenvalue

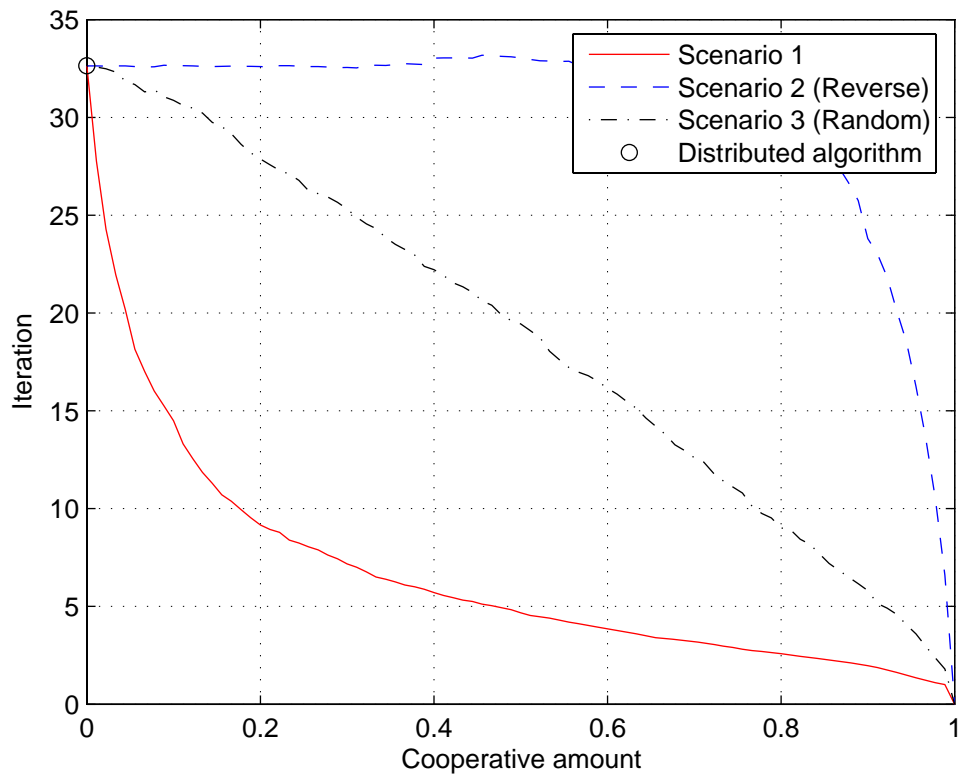


Figure 4.2: The number of iterations with cooperation

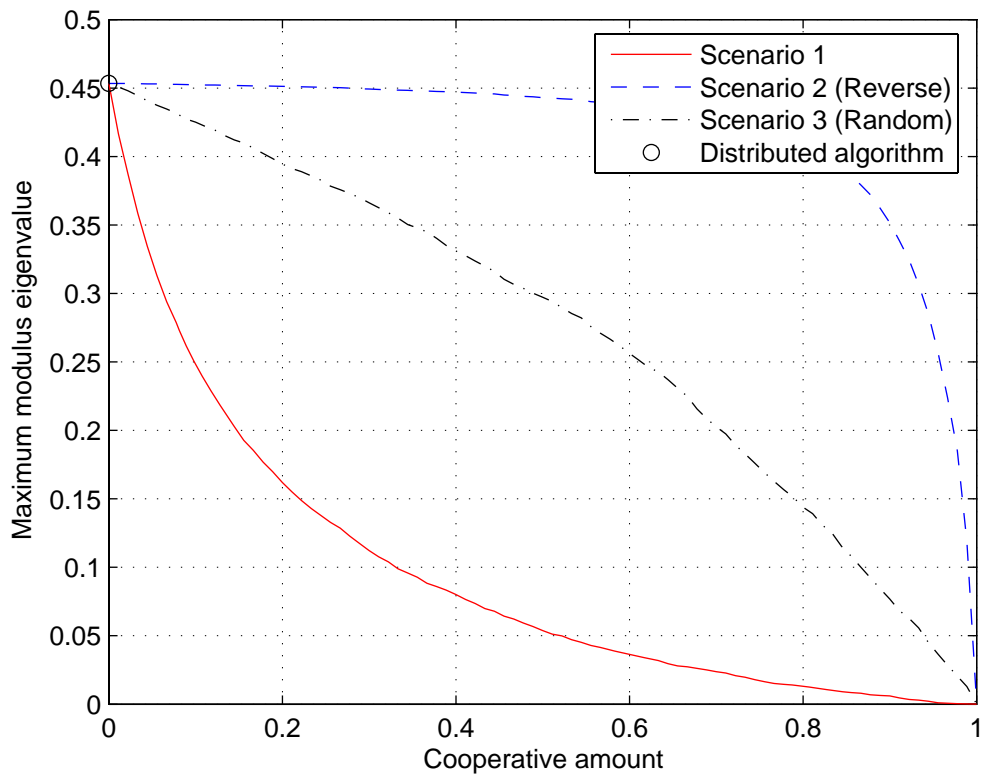


Figure 4.3: The maximum modulus eigenvalue with cooperation

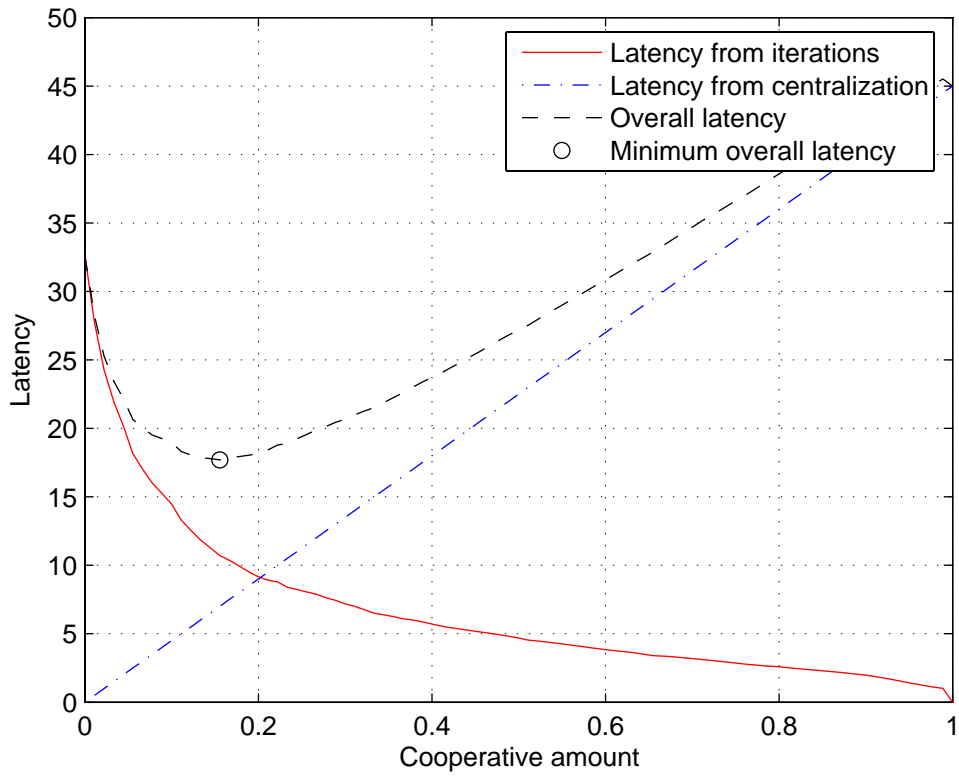


Figure 4.4: The overall latency with cooperation

analysis that not all the cross-link gains in a cooperative group have to be identified and shared; using any of them reduces the maximum modulus eigenvalue of the matrix updating power vector. The simulation results show that the greater cross-link gains contribute the greater enhancement to the convergence speed. Since these are the ones that would be easiest to measure in practice, the result is felicitous.

The convergence time is reduced from one of the distributed algorithm to one of the centralized algorithm ( $= 1$ ) as the identified and shared cross-link gains increases from 0 to  $M^2 - M$ . A simple and realistic cooperation scenario is introduced. It was shown that with only 10% cooperation the convergence speed of the distributed power control algorithm is doubled.

This cooperative power control algorithm can be thought as a general form of power control from the distributed to the centralized power control algorithm. It is realized that a local centralizing infrastructure or limited opportunity of centralization can beneficially be used for power control. It is possible to compare the latencies for the centralization and iterations and make an optimal decision regarding the degree of cooperation to employ.

# Chapter 5

## Dynamic Resource Allocation with Low Complexity for Real Time Traffic in Uplink OFDMA Systems

### 5.1 Introduction

Orthogonal frequency division multiple access (OFDMA) is one of the most promising multiple access schemes for broadband wireless networks. Since OFDMA is capable of achieving high spectral efficiency even in multiuser environments, it is an adequate scheme for real time (RT) traffic requiring high data rate that increasingly dominates current wireless systems. In this chapter we consider problems of resource allocation in single-cell networks, or larger networks in which the cells do not coordinate allocation decisions with each other (e.g., WiFi).

Downlink resource allocation (DRA) in OFDMA systems has been widely investigated in order to maximize sum-rate [44]–[47] or minimize total transmitting power [47]–[50] with consideration of minimum rate constraints. Since power constraints are

distributed for individual users in the uplink, the DRA algorithms cannot be directly applied. The optimality of uplink OFDMA systems is studied in [51], and efficient uplink resource allocation (URA) algorithms have been proposed in [52]–[54]. Kim et al. [52] showed that each subcarrier should be exclusively allocated to a user who has the maximum marginal rate value with the subcarrier in order to maximize sum-rate. Gao and Cui [53] improved Kim’s algorithm with fairness considerations. Ng and Sung [54] generalized the URA problem with utility functions.

Even though efficient URA algorithms achieve a remarkable reduction in complexity compared to optimal resource allocation, their complexities are still heavy since they compute the marginal rate (or utility) values for every user to make a single decision for each subcarrier, and the number of subcarriers is usually very large.

The efficient URA algorithms in [52]–[54] show near-optimal performance with satisfying Karush-Huhn-Tucker (KKT) conditions which are necessary to solve relaxed optimal problems. They, however, focus on maximization of sum-rate (or utility) but do not strongly consider other common QoS requirements. Therefore, even though they reduce complexity with acceptable degradation of the sum-rate (the objective function), the degradation of QoS (the constraints functions) may not be acceptable. For example, Gao and Cui [53] considered the QoS requirements with a two-step URA algorithm of initial allocation that assigns subcarriers only to users whose rates are below their targets and residual allocation that assigns the rest of the subcarriers to further increase the sum rate. This approach improves outage probability for users with QoS constraints with small modification of previous works, but the outage probability may not be good enough to satisfy QoS requirements of RT traffic.

In this chapter, we propose a very efficient dynamic URA algorithm which focuses on the QoS requirements for RT traffic. We suggest a user-by-user dynamic resource allocation with a simple prioritization in uplink OFDMA systems. It has even less

complexity than the conventional channel-by-channel URA algorithms and gives better QoS for RT traffic. In addition, with an appropriate protocol, the proposed algorithm can be performed in a distributed way with simple information exchanges between a Base Station (BS) and its users.

The rest of the chapter is organized as follows. In Section 5.2, we describe the system model and formulate resource allocation problems. The proposed algorithm is introduced in Section 5.3. In Section 5.4, simulation results are shown. We conclude in Section 5.5.

## 5.2 System Model and Problem Formulation

We consider an uplink OFDMA system with  $K$  users and  $N$  subcarriers. The achievable rate of the  $i$ th user at time index  $k$  is given by

$$R_i(k) = \sum_{j=1}^N x_{ij}(k) \log_2 \left( 1 + \frac{G_{ij}(k)P_{ij}(k)}{\eta_{ij}(k)} \right), \quad i = 1, \dots, K, \quad (5.1)$$

where  $G_{ij}(k)$  is the channel gain,  $P_{ij}(k)$  is the allocated transmitting power,  $\eta_{ij}(k)$  is the noise power on subcarrier  $j$  of the  $i$ th user, and the binary decision variable at time index  $k$ ,  $x_{ij}(k)$ , is defined as

$$x_{ij}(k) = \begin{cases} 1, & \text{if the subcarrier } j \text{ is allocated to } i\text{th user} \\ 0, & \text{otherwise} \end{cases}. \quad (5.2)$$

We mainly consider the performance of RT traffic in this chapter. The service outage probability is defined as

$$p_i^{\text{out}}(k) \equiv \text{Prob} \left( R_i(k) < R_i^{\text{target}} \right), \quad i = 1, \dots, K, \quad (5.3)$$

where  $R_i^{\text{target}}$  is the target rate of the  $i$ th user which must be supported for its QoS requirement. The resource allocation problems are formulated for the average perfor-

mance as

$$\begin{aligned}
 & \min_{x_{ij}(k)} \quad \sum_{i=1}^K p_i^{\text{out}}(k) \\
 \text{s. t.} \quad & \sum_{j=1}^N P_{ij}(k) \leq P_i^{\text{max}} \quad , \quad i = 1, \dots, K \quad , \\
 & \sum_{i=1}^K \sum_{j=1}^N x_{ij}(k) = N
 \end{aligned} \tag{5.4}$$

and for the min-max performance as

$$\begin{aligned}
 & \min_{x_{ij}(k)} \quad \max_i \sum_k p_i^{\text{out}}(k) \\
 \text{s. t.} \quad & \sum_{j=1}^N P_{ij}(k) \leq P_i^{\text{max}} \quad i = 1, \dots, K \quad , \\
 & \sum_{i=1}^K \sum_{j=1}^N x_{ij}(k) = N
 \end{aligned} \tag{5.5}$$

where  $k$  is the time index and  $P_i^{\text{max}}$  is the total power of the  $i$ th user.

### 5.3 Proposed Algorithm

In DRA algorithms, each subcarrier is allocated to a user who has the best channel condition among all users to maximize sum-rate. Similarly in most efficient URA algorithms, each subcarrier is sequentially allocated to a user who has the maximum marginal rate value with the subcarrier [52] since each user has different power constraints and modulation adaptabilities. This conventional URA algorithm has the result that users who do not have the best channel conditions among all users cannot occupy any subcarrier, and thus they cannot meet their QoS requirements. Fairness is considered with the two-step allocations in [53] of initial and residual allocations. In the initial allocation procedure, users who meet their QoS requirements are excluded and only the rest of the users keep competing. This two-step allocation gives higher priorities to the users who do not meet their QoS requirements and improves the fairness.

However, there still remains a problem since it is possible that a subcarrier allocated to a user (i.e., the user's channel condition of the subcarrier is best among all

users) is the worst subcarrier of the user. That is, even if the user has many better subcarriers among the remaining unallocated subcarriers, a bad subcarrier may be allocated to the user when all other users' channel conditions of the subcarrier are worse. This is a common problem of downlink and uplink systems if fairness is considered.

Moreover, due to the distributed nature of power constraints in the uplink, a decision of one subcarrier allocation has a big effect on the decision for the next subcarrier allocation. If some subcarriers are allocated to a user, then its utility increment for another subcarrier will be limited. Therefore even if there remains a subcarrier among the unallocated remaining subcarriers that the channel condition is the best among all subcarriers for the user and also the best among all users, the possibility that the user occupies the subcarrier becomes smaller if some other subcarriers are already allocated to the user. Consequently, one wrong decision can result in significant sub-optimality in the conventional efficient URA algorithms.

For these reasons, conventional efficient algorithms designed for the downlink in which all users share total power may not be good for an uplink subject to a fairness requirement. Some alternative utility functions for proportional fairness and max-min fairness are suggested in [54]. But for the same reasons, fairness is still hard to guarantee with sequential allocation per subcarrier.

This problem can be thought as a conflict between multi-user diversity and the multi-channel diversity of each user. We propose a dynamic URA algorithm with sequential allocation per user rather than per subcarrier, obtaining multi-channel diversity of each user with generous subcarrier occupation (large number of bits) in order to preserve the multi-user diversity as much as possible. Given the target rate, the generous subcarrier occupation of each user with multi-channel diversity tends to free more resources for other users. In addition, a strategy for long-term fairness is

considered using the capability of simple and explicit prioritization of the proposed algorithm.

### 5.3.1 Power Allocation

The well-known “water-filling” power allocation among subcarriers is considered in this chapter. For the uplink, the “water-filling” does not have much computational burden: the “water level” is easily calculated for each user because the power is not shared among users and the maximum power level is predetermined for each user in contrast to downlink. The “water-filling” power allocation is explained as

$$P_{ij} = x_{ij} \left[ \nu_i - \frac{G_{ij}}{\eta_{ij}} \right]^+, \quad (5.6)$$

where  $[y]^+ = \max(y, 0)$  and  $\sum_{j=1}^N P_{ij} = P_i^{\max}$ . Equal power allocation is compared to the water-filling power allocation in [52]. In [53], the rate increment values in the subcarrier allocation procedure are calculated based on equal power allocation. The water-filling power allocation is performed in the actual power allocation phase to reduce complexity. In this chapter also, equal power allocation is considered in the prioritizing stage and water-filling power allocation is considered in the subcarrier allocation.

### 5.3.2 Subcarrier Allocation

We suggest two types of cost functions to minimize average and maximum outage performance. For minimizing the average outage performance, an appropriate cost measure is the number of required subcarriers to meet QoS constraints. A simple approximation is that the cost of the  $i$ th user at time  $k$  is given by

$$C_i^{\text{MA}}(k) = \frac{R_i^{\text{target}}}{\text{maximum achievable rate at time } k}. \quad (5.7)$$

For minimizing the maximum outage performance, the appropriate cost measure is the outage performance until the current time. It is given by

$$C_i^{\text{MM}}(k) = -(\text{servie outage time until time } k). \quad (5.8)$$

The resource allocation procedure is as follows:

Table 5.1: Proposed URA algorithm

---



---

Step 1:	Calculate cost values for all users.
Step 2:	Assign the highest priority to the user with the minimum cost value.
Step 3:	Allocate the minimum number of required subcarriers to the highest prioritized user.
Step 4:	Repeat Step 3 for the remaining users with unallocated subcarriers.

---



---

If there are not enough subcarriers remaining to meet the QoS requirement in Step 3, the user does not occupy any subcarriers and is excluded in the allocation procedure at that time (i.e., service outage).

### 5.3.3 Complexity

Given the channel conditions of all subcarriers for all users, only one computation for the maximum achievable rate (5.7) of each user is needed in Step 1. In Step 3 and 4, the total computations for the water-filling power allocation for all successful users cannot exceed  $N$ . Let  $K_{\text{out}}$  the number of users who do not occupy any subcarriers. Even if the computations for all  $K_{\text{out}}$  users are performed before all subcarriers are allocated (i.e., before the algorithm is finished), then the total computation for the  $K_{\text{out}}$  users cannot exceed  $N \times K_{\text{out}}$ . Therefore, the worst case complexity of the proposed algorithm is bounded by  $O(K + N + N \times K_{\text{out}})$ . Since  $K_{\text{out}}$  is usually very small, it approaches  $O(K + N)$ . Only in a case of extremely heavy loading (i.e.,  $K \approx$

$K_{\text{out}}$ ), it will be close to  $O(K \times N)$ . Therefore, in realistic situations, the complexity of the proposed dynamic URA algorithm is much less than the conventional URA algorithms,  $O(K \times N)$  or  $O(K \times N^2)$  [53].

Moreover, the proposed algorithm can be performed in a distributed way with an appropriate protocol:

Table 5.2: A protocol for distributed implementation of the proposed URA algorithm

- 
- Step 1: Each user calculates its own cost and reports it to its BS.
  - Step 2: BS prioritizes the users.
  - Step 3: BS sends a list of unoccupied subcarriers to the highest prioritized user or broadcasts the list to all users.
  - Step 4: The highest prioritized user occupies the minimum number of subcarriers among the unoccupied subcarriers to meet its QoS requirement.
  - Step 5: Repeat Steps 3 and 4.
- 

Based on this protocol, resource allocation can be performed by exchanging a small amount of information comprised of cost values, priorities and lists of unoccupied subcarriers. The protocol also distributes the computational burden among the users.

## 5.4 Simulation Results

50 subcarriers and randomly placed users are considered in a circular cell with 100m radius. The channel gains are modeled with the path loss exponent 4, the shadowing with a mean of 0dB and a standard deviation of 8dB, and the receiver noise level of -174dBm. The maximum transmitting power is constrained as 200dB. The users are assumed immobile during the time a traffic flow is served. The resource allocation algorithm is performed every frame, each of duration  $T$ . The rate targets for RT traffic are set to 0.5 and 1Mbps and randomly assigned to users. The service time for

the RT traffic is set as  $1000T$ . 10,000 independent experiments are performed and averaged for each result as we vary the number of users.

The averaged and the maximum service outage performances are shown in Figs. 5.1 and 5.2. The proposed algorithm with two kinds of cost functions,  $C^{\text{MA}}$  in (5.7) and  $C^{\text{MM}}$  in (5.8), are compared to the conventional URA algorithms with three different utility functions for throughput optimization (TO), proportional fairness (PF) and max-min fairness (Max-min) in [54]. It is shown that the proposed algorithm outperforms the conventional algorithms with much reduced complexity. The proposed algorithm with  $C^{\text{MA}}$  gives the best average outage performance (38% ~ 53% better than TO) and one with  $C^{\text{MM}}$  also outperforms the conventional algorithms for the average outage performance (24% ~ 53% better than TO). The proposed algorithm with  $C^{\text{MM}}$  shows the best maximum outage performance with large gaps from others (36% ~ 79% better than TO).

## 5.5 Conclusion

In this chapter, we proposed an efficient dynamic resource allocation algorithm for RT traffic in uplink OFDMA systems. In contrast to the conventional URA algorithms performing computations for each subcarrier, the proposed algorithm performs computations for each user. Since the number of users who do not satisfy their QoS requirements is usually quite small, the proposed algorithm contributes a large reduction of the complexity from  $O(K \times N)$  or  $O(K \times N^2)$  to  $O(K + N)$ . If most users cannot meet their QoS requirements with the extremely high loading, then the complexity approaches the simplest of the conventional algorithms. With the proposed protocols, the computational complexity can be distributed to users with a small amount of information exchange. In addition to the complexity reduction, the proposed algorithm outperforms the conventional URA algorithms for RT traffic.

Not only the average outage performance, but also the long-term maximum outage performance is improved since it is possible to control fairness among users directly in the proposed algorithm.

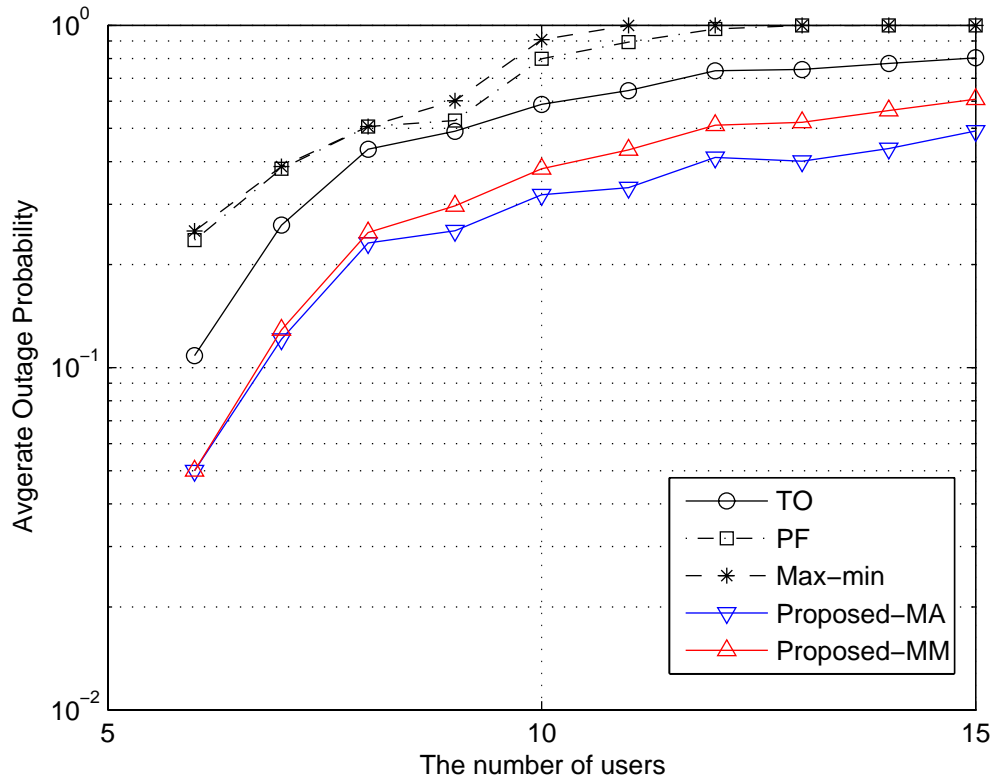


Figure 5.1: Average outage probability

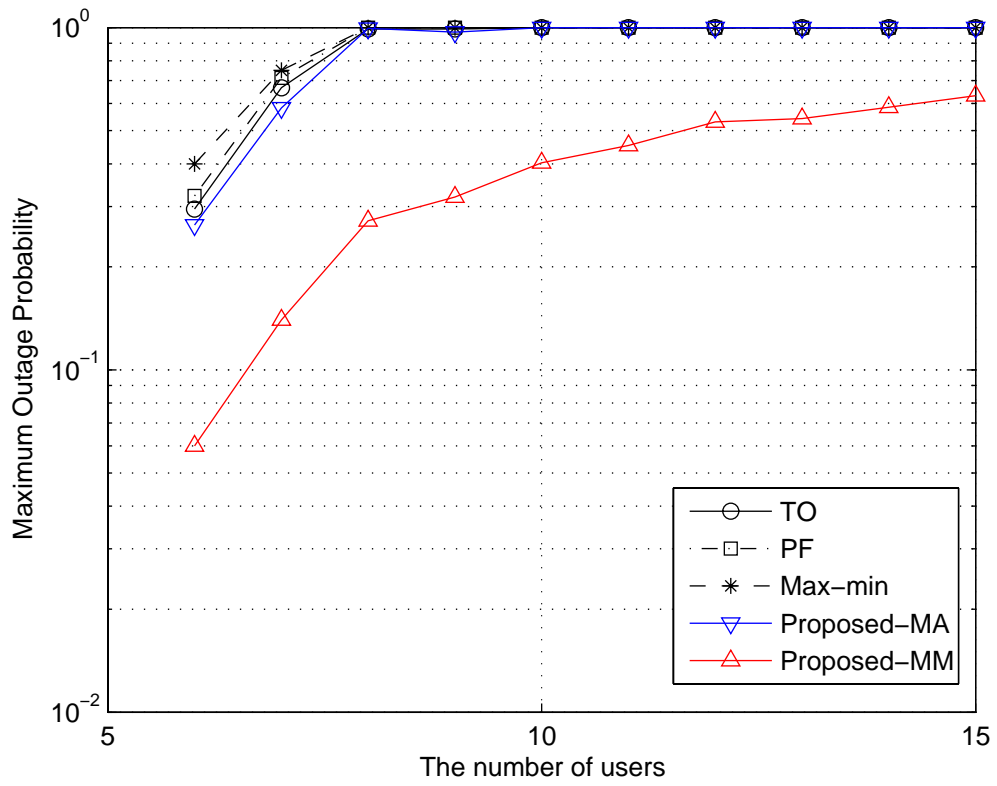


Figure 5.2: Maximum outage probability

# Chapter 6

## Conclusion and Future Works

### 6.1 Conclusion

We focus on the costs and benefits of different degrees of cooperation among users and controllers in gathering and exchanging channel and interference state information. Cooperative strategies and algorithms for various wireless network systems are studied.

In Chapter 3, the reduction of relay node density with cooperative actions of nodes is shown while the QoS is preserved. The gain is mainly derived from the benefit of the path diversity which is induced by the cooperation among nodes. At the low end of the potential gains, implementation losses and the considerable increase in complexity argue that simple relay strategies are probably sufficient. At the higher end, the research suggests there is value in pursuing practical algorithms to effect the cooperation.

In Chapter 4, we proposed a cooperative power control algorithm targeted mainly at cellular networks. We proved that the cooperation enhances the convergence speed. The cooperative power control algorithm is represented as a general form of power control from the distributed to the centralized power control algorithm. A local

centralizing infrastructure or limited opportunity of centralization can beneficially be used for power control. It is possible to compare the latencies for the centralization and iterations and make an optimal decision regarding the degree of cooperation to employ.

In Chapter 5, our attention turned to single-cell networks. We proposed an efficient dynamic resource allocation algorithm for RT traffic in uplink OFDMA systems. In contrast to the conventional URA algorithms performing computations for each subcarrier, the proposed algorithm performs computations for each user and the proposed algorithm contributes a large reduction to the complexity. With the proposed protocols, the computational complexity can be distributed to users with a small amount of information exchange. In addition to the complexity reduction, the proposed algorithm outperforms the conventional URA algorithms for RT traffic. Not only the average outage performance, but also the long-term maximum outage performance is improved since it is possible to control fairness among users directly in the proposed algorithm. The benefits of the proposed algorithm on the complexity and performance are derived from the multi-channel diversity which has been ignored while the conventional algorithms are concentrating on the multi-user diversity.

## 6.2 Future Works

One of the major difficulties in OFDMA systems is inter-cell interference (ICI) control even though the intra-cell interferences are completely avoided by exclusive sub-carrier allocation to users. A conventional way to control the ICI is introduced in [54]. They suggest a hierarchical coordination by Radio Network Controller (RNC) and BSs. Even though they assume that the RNC allocates sub-carriers to cells in each super-frame given the channel information of users no matter whether they have packets to send and BSs allocate the assigned sub-carriers to each user who really

has packets to send in their cells, the complexity is still dominated by the utility-comparison/allocation per subcarrier approach. The complexities of the processes at the RNC and BS are  $O(L \times K \times N)$  and  $O(K_i \times N_i)$  respectively where  $L$  is the number of BSs, and  $K_i$  and  $N_i$  are the number of users and the number of subcarriers for the  $i$ th BS. We believe that the proposed algorithm can contribute to a reduction in the complexities for the  $i$ th RNC and BSs while yielding better outage for RT traffic. However, the benefits have yet to be quantified in simulation.

Jointly with the cooperative power control introduced in Chapter 4, the network capacity can be improved more effectively for a heterogeneous traffic condition. For delay-tolerant traffic, the cooperative power control can be implemented, and the cooperation level can be decided to minimize the total network latency given infrastructure and opportunities for centralization or cooperation. For delay-sensitive traffic which requires an immediate decision of resource allocation, the efficient resource allocation algorithm introduced in Chapter 5 will provide an acceptable QoS. Due to the very low complexity of the algorithm, it can be more attractive for coordination of multi-cell networks.

The dynamics for decisions and implementation of various strategies according to traffic types, channel conditions, given infrastructure, capability of cooperation and so on in a network will be an important factor in improving the network capacity. Explosively increasing demands of wireless access expand the heterogeneity to all aspects of wireless communications environments. We believe that this dissertation can contribute deciding on the dynamics that the future wireless systems have to achieve.

# Appendix A

## APPENDIX for Proofs of Theorems

### A.1 Proof of Theorem 1

Define the  $M \times M$  matrix  $\mathbf{F}_{c0} = \begin{pmatrix} \mathbf{F}_c & \mathbf{0}_{n \times (M-n)} \\ \mathbf{0}_{(M-n) \times n} & \mathbf{0}_{(M-n) \times (M-n)} \end{pmatrix}$ , and let  $\beta$  be the eigenvalue of  $\mathbf{F}_{c0}$ . Since  $0 \leq \mathbf{F}_{c0} \leq \mathbf{F}$ , then  $|\beta| \leq \hat{\lambda}(\mathbf{F})$  (Theorem 1.5.e in [43]). When the feasible power vector  $\mathbf{P}^* = (\mathbf{I} - \mathbf{F})^{-1} \mathbf{u}$  exists,  $\hat{\lambda}(\mathbf{F}) < 1$  (Theorem 2.1 in [43]) and  $|\beta| < 1$ . Thus the eigenvalue of  $\mathbf{I} - \mathbf{F}_{c0}$  is  $1 - \beta$  and non-zero. Therefore an eigenvalue of  $\mathbf{I}_n - \mathbf{F}_c$  cannot be zero also where  $\mathbf{I}_n$  is the  $n \times n$  identity matrix, i.e.,  $\mathbf{I}_n - \mathbf{F}_c$  is invertible. Q.E.D.

### A.2 Proof of Theorem 2

Proved by (A.13) in APPENDIX A.3.

### A.3 Proof of Theorem 3

If the cooperative algorithm (4.21) with a network cooperation matrix  $\mathbf{C}$  converges to the Pareto optimal solution, then

$$\widehat{\lambda}(\mathbf{I} - (\mathbf{I} - \mathbf{C})^{-1}(\mathbf{I} - \mathbf{F})) = \rho < 1. \quad (\text{A.1})$$

Let the associated eigenvector  $y$  with  $\rho$ , then from (4.5) and [43],

$$(\mathbf{I} - (\mathbf{I} - \mathbf{C})^{-1}(\mathbf{I} - \mathbf{F}))y - \rho y = 0 \quad \text{and} \quad y > 0. \quad (\text{A.2})$$

If there exist a vector  $z \in X_+$  such that

$$\left(\mathbf{I} - (\mathbf{I} - \mathbf{C}^+)^{-1}(\mathbf{I} - \mathbf{F})\right)z - \rho z < 0, \quad \text{then} \cdot \quad (\text{A.3})$$

$$\widehat{\lambda}\left(\mathbf{I} - (\mathbf{I} - \mathbf{C}^+)^{-1}(\mathbf{I} - \mathbf{F})\right) < \widehat{\lambda}(\mathbf{I} - (\mathbf{I} - \mathbf{C})^{-1}(\mathbf{I} - \mathbf{F})) = \rho < 1. \quad (\text{A.4})$$

Let  $z = (\mathbf{I} - \mathbf{F})^{-1}(\mathbf{I} - \mathbf{C}^+)y$ , where

$$(\mathbf{I} - \mathbf{F})^{-1}(\mathbf{I} - \mathbf{C}^+) = \left[(\mathbf{I} - \mathbf{C}^+)^{-1}(\mathbf{I} - \mathbf{F})\right]^{-1} = \sum_{k=0}^{\infty} \left[\mathbf{I} - (\mathbf{I} - \mathbf{C}^+)^{-1}(\mathbf{I} - \mathbf{F})\right]^k, \quad (\text{A.5})$$

then

$$(\mathbf{I} - \mathbf{F})^{-1}(\mathbf{I} - \mathbf{C}^+) = (\mathbf{I} - \mathbf{F})^{-1}(\mathbf{I} - \mathbf{F} + \mathbf{F} - \mathbf{C}^+) = \mathbf{I} + (\mathbf{I} - \mathbf{F})^{-1}(\mathbf{F} - \mathbf{C}^+), \quad (\text{A.6})$$

$(\mathbf{I} - \mathbf{F})^{-1} > 0$  (Theorem 2.1 and its corollary in [43]) and  $(\mathbf{F} - \mathbf{C}^+) \geq 0$  by (4.19).

Thus  $(\mathbf{I} - \mathbf{F})^{-1}(\mathbf{I} - \mathbf{C}^+) = \mathbf{I} + (\mathbf{I} - \mathbf{F})^{-1}(\mathbf{F} - \mathbf{C}^+) \geq 0$  with no zero row (and column) and  $y > 0$ , and

$$z = (\mathbf{I} - \mathbf{F})^{-1}(\mathbf{I} - \mathbf{C}^+)y > 0, \quad \text{i.e.,} \quad z \in X_+. \quad (\text{A.7})$$

From (A.2), an equation is derived as

$$(\mathbf{I} - \mathbf{F})y = (1 - \rho)(\mathbf{I} - \mathbf{C})y. \quad (\text{A.8})$$

Using (A.7) and (A.8), the left-hand side of (A.3) is

$$\begin{aligned}
& \left( \mathbf{I} - (\mathbf{I} - \mathbf{C}^+)^{-1} (\mathbf{I} - \mathbf{F}) \right) z - \rho z \\
&= \left( \mathbf{I} - (\mathbf{I} - \mathbf{C}^+)^{-1} (\mathbf{I} - \mathbf{F}) \right) (\mathbf{I} - \mathbf{F})^{-1} (\mathbf{I} - \mathbf{C}^+) y \\
&\quad - \rho (\mathbf{I} - \mathbf{F})^{-1} (\mathbf{I} - \mathbf{C}^+) y \\
&= (\mathbf{I} - \mathbf{F})^{-1} (\mathbf{I} - \mathbf{C}^+) \left[ \left( \mathbf{I} - (\mathbf{I} - \mathbf{C}^+)^{-1} (\mathbf{I} - \mathbf{F}) \right) y - \rho y \right] \\
&= (\mathbf{I} - \mathbf{F})^{-1} (\mathbf{I} - \mathbf{C}^+) \left[ (1 - \rho) y - (1 - \rho) (\mathbf{I} - \mathbf{C}^+)^{-1} (\mathbf{I} - \mathbf{C}) y \right], \tag{A.9} \\
&= (1 - \rho) (\mathbf{I} - \mathbf{F})^{-1} (\mathbf{I} - \mathbf{C}^+) \left[ \mathbf{I} - (\mathbf{I} - \mathbf{C}^+)^{-1} (\mathbf{I} - \mathbf{C}) \right] y \\
&= (1 - \rho) (\mathbf{I} - \mathbf{F})^{-1} [(\mathbf{I} - \mathbf{C}^+) - (\mathbf{I} - \mathbf{C})] y \\
&= (1 - \rho) (\mathbf{I} - \mathbf{F})^{-1} (\mathbf{C} - \mathbf{C}^+) y
\end{aligned}$$

where

$$(1 - \rho) > 0, \quad (\mathbf{I} - \mathbf{F})^{-1} > 0, \quad (\mathbf{C} - \mathbf{C}^+) \leq 0, \quad (\mathbf{C} - \mathbf{C}^+) \neq 0, \quad \text{and} \quad y > 0. \tag{A.10}$$

Since the vector in the last line of (A.9) satisfies  $(\mathbf{C} - \mathbf{C}^+) y \leq 0$  and  $(\mathbf{C} - \mathbf{C}^+) y \neq 0$  by (A.10), it is derived as

$$\left( \mathbf{I} - (\mathbf{I} - \mathbf{C}^+)^{-1} (\mathbf{I} - \mathbf{F}) \right) z - \rho z = (1 - \rho) (\mathbf{I} - \mathbf{F})^{-1} (\mathbf{C} - \mathbf{C}^+) y < 0. \tag{A.11}$$

Therefore,

$$\widehat{\lambda} \left( \mathbf{I} - (\mathbf{I} - \mathbf{C}^+)^{-1} (\mathbf{I} - \mathbf{F}) \right) < \rho < 1. \quad \text{Q.E.D.} \tag{A.12}$$

Using Theorem 3, Theorem 2 is proved as,

$$\widehat{\lambda} (\mathbf{I} - (\mathbf{I} - \mathbf{C})^{-1} (\mathbf{I} - \mathbf{F})) < \widehat{\lambda} (\mathbf{I} - (\mathbf{I} - \mathbf{0})^{-1} (\mathbf{I} - \mathbf{F})) = \widehat{\lambda} (\mathbf{F}) < 1. \tag{A.13}$$

# Bibliography

- [1] T. S. Rappaport, *Wireless Communications: Principles and Practice*, 2nd ed., Upper Saddle River, NJ: Prentice Hall, 2002.
- [2] M. J. Feuerstein, K. L. Blackard, T. S. Rappaport, S. Y. Seidel, and H. H. Xia, “Path loss, delay spread, and outage models as functions of antenna height for microcellular system design,” *IEEE Trans. Veh. Technol.*, vol. 43, no. 3, pp. 487–498, Aug. 1994.
- [3] A. Leon-Garcia, *Probability and Random Processes for Electrical Engineering*, 2nd ed., Addison-Wesley Publishing Company, Inc., 1994.
- [4] W. C. Y. Lee, *Mobile Communications Design Fundamentals*, New York, NY: John Wiley & Sons, Inc., 1992.
- [5] C. K. Toh, *Ad Hoc Mobile Wireless Networks: Protocols and Systems*, Englewood Cliffs, NJ: Prentice Hall, 2001.
- [6] F. Li and Y. Wang, “Routing in vehicular ad hoc networks: a survey,” *IEEE Veh. Technol. Mag.*, vol. 2, no. 2, pp. 12–22, June 2007.
- [7] L. Hanzo-II and R. Tafazolli, “A survey of QoS routing solutions for mobile ad hoc networks,” *IEEE Commun. Surveys & Tutorials*, vol. 9, no. 2, pp. 50–70, 2007.

- [8] L. Chen and W. B. Heinzelman, “A survey of routing protocols that support QoS in mobile ad hoc networks,” *IEEE Network*, vol. 21, no. 6, pp. 30–38, Nov. 2007.
- [9] P. Gupta and P. R. Kumar, “The capacity of wireless networks,” *IEEE Trans. Inf. Theory*, vol. 46, no. 2, pp. 388–404, Mar. 2000.
- [10] A. Nosratinia, T. E. Hunter, and A. Hedayat, “Cooperative communication in wireless networks,” *IEEE Commun. Mag.*, vol. 42, no. 10, pp. 74–80, Oct. 2004.
- [11] J. Heiskala and J. Terry, *OFDMA Wireless LANs: A Theoretical and Practical Guide*, SAMS Publishing, 2004.
- [12] T. Cover and A. E. Gamal, “Capacity theorems for the relay channel,” *IEEE Trans. Inf. Theory*, vol. 25, no. 5, pp. 572–584, Sept. 1979.
- [13] A. Sendonaris, E. Erkip, and B. Aazhang, “User cooperation diversity-Part I: system description,” *IEEE Trans. Commun.*, vol. 51, no. 11, pp. 1927–1938, Nov. 2003.
- [14] —, “User cooperation diversity-Part II: Implementation aspects and performance analysis,” *IEEE Trans. Commun.*, vol. 51, no. 11, pp. 1939–1948, Nov. 2003.
- [15] J. N. Laneman, D. N. C. Tse, and G. W. Wornell, “Cooperative diversity in wireless networks: Efficient protocols and outage behavior,” *IEEE Trans. Inf. Theory*, vol. 50, no. 12, pp. 3062–3080, Dec. 2004.
- [16] J. N. Laneman, G. W. Wornell, and D. N. C. Tse, “An efficient protocol for realizing cooperative diversity in wireless networks,” *Proc. IEEE ISIT*, Washington DC, pp. 294, June 2001.

- [17] G. Kramer, M. Gastpar, and P. Gupta, “Cooperative strategies and capacity theorems for relay networks,” *IEEE Trans. Inf. Theory*, vol. 51, no. 9, pp. 3037–3063, Sept. 2005.
- [18] T. E. Hunter and A. Nosratinia, “Diversity through coded cooperation,” *IEEE Trans. Wireless Commun.*, vol. 5, no. 2, pp. 283–289, Feb. 2006.
- [19] A. Stefanov and E. Erkip, “Cooperative coding for wireless networks,” *IEEE Trans. Commun.*, vol. 52, no. 9, pp. 1470–1476, Sept. 2004.
- [20] M. Janani, A. Hedayat, T. E. Hunter, and A. Nosratinia, “Coded cooperation in wireless communications: Space-time transmission and iterative decoding,” *IEEE Trans. Signal Process.*, vol. 52, no. 2, pp. 362–371, Feb. 2004.
- [21] J. N. Laneman and G. W. Wornell, “Distributed space-time-coded protocols for exploiting cooperative diversity in wireless networks,” *IEEE Trans. Inf. Theory*, vol. 49, no. 10, pp. 2415–2425, Oct. 2003.
- [22] H. Ochiai, P. Mitran, H.V. Poor, and V. Tarokh, “Collaborative beamforming for distributed wireless ad hoc sensor networks,” *IEEE Trans. Signal Process.*, vol. 53, no. 11, pp. 4110–4124, Nov. 2005.
- [23] L. Dong, A. P. Petropulu, and H. V. Poor, “A cross-layer approach to collaborative beamforming for wireless ad hoc networks,” *IEEE Trans. Signal Process.*, vol. 56, no. 7, pp. 2981–2993, July 2008.
- [24] A. Scaglione and Y. W. Hong, “Opportunistic large arrays: cooperative transmission in wireless multihop ad hoc networks to reach far distances,” *IEEE Trans. Signal Process.*, vol. 51, no. 8, pp. 2082–2092, Aug. 2003.
- [25] S. Wei, D. L. Goeckel, and M. C. Valenti, “Asynchronous cooperative diversity,” *IEEE Trans. Wireless Commun.*, vol. 5, no. 6, pp. 1547–1557, June 2006.

- [26] X. Li, "Space-time coded multi-transmission among distributed transmitters without perfect synchronization," *IEEE Signal Process. Lett.*, vol. 11, no. 12, pp. 948–951, Dec. 2004.
- [27] P. Liu, Z. Tao, Z. Lin, E. Erkip, and S. Panwar, "Cooperative wireless communications: a cross-layer approach," *IEEE Wireless Commun.*, vol. 13, no. 4, pp. 84–92, Aug. 2006.
- [28] A. J. Paulraj, D. A. Gore, R. U. Nabar and H. Bolcskei, "An overview of MIMO communications- a key to gigabit wireless," *Proc. IEEE*, vol. 92, no. 2, pp. 198–218, Feb. 2004.
- [29] T. M. Cover and J. A. Thomas, *Elements of Information Theory*, New York: Wiley, 1991.
- [30] E. Telatar, "Capacity of multi-antenna Gaussian channels," *Eur. Trans. Tel.*, vol. 10, no. 6, pp. 585–595, Nov./Dec. 1999.
- [31] G. J. Foschini and M. J. Gans, "On limits of wireless communication in a fading environment when using multiple antennas," *Wireless Personal Commun.*, vol. 6, no. 3, pp. 311–335, Mar. 1998.
- [32] A. Goldsmith, S. A. Jafar, N. Jindal, and S. Vishwanath, "Capacity limits of MIMO channels," *IEEE J. Sel. Areas Commun.*, vol. 21, no. 5, pp. 684–702, June 2003.
- [33] N. Jindal, U. Mitra and A. Goldsmith, "Capacity of ad-hoc networks with node cooperation," *Proc. IEEE ISIT 2004*, pp. 271, June 2004.
- [34] M. Kang and M. S. Alouini, "Capacity of MIMO Rician channels," *IEEE Trans. Wireless Commun.*, vol. 5, no. 1, pp. 112–122, Jan 2006.

- [35] S. K. Jayaweera and H. V. Poor, "On the capacity of multiple-antenna systems in Rician fading," *IEEE Trans. Wireless Commun.*, vol. 4, no. 3, pp. 1102–1111, May 2005.
- [36] N. Balakrishnan and A. C. Cohen, *Order Statistics and Inference*, New York: Academic Press, 1991.
- [37] J. Zander, "Performance of optimum transmitter power control in cellular radio systems," *IEEE Trans. Veh. Technol.*, vol. 41, no. 1, pp. 57–62, Feb. 1992.
- [38] S. A. Grandhi, R. Vijayan, D. J. Goodman, and J. Zander, "Centralized power control in cellular radio systems," *IEEE Trans. Veh. Technol.*, vol. 42, no. 4, pp. 466–468, Nov. 1993.
- [39] G. J. Foschini and Z. Miljanic, "A simple distributed autonomous power control algorithm and its convergence," *IEEE Trans. Veh. Technol.*, vol. 42, no. 4, pp. 641–646, Nov. 1993.
- [40] D. Mitra, "An asynchronous distributed algorithm for power control in cellular radio systems," *Proc. 4th WINLAB Workshop*, pp. 249–259, 1993.
- [41] S. A. Grandhi, J. Zander, and R. Yates, "Constrained power control," *Wireless Personal Commun.*, vol. 1, no. 4, pp. 257–270, Dec. 1994.
- [42] N. Bambos, S. C. Chen, and G. J. Pottie, "Channel access algorithms with active link protection for wireless communication networks with power control," *IEEE/ACM Trans. Netw.*, vol. 8, no. 5, pp. 583–597, Oct. 2000.
- [43] E. Seneta, *Non-Negative Matrices*, Halsted Press, 1973.

- [44] M. Ergen, S. Coleri, and P. Varaiya, “QoS aware adaptive resource allocation techniques for fair scheduling in OFDMA based broadband wireless access systems,” *IEEE Trans. Broadcast.*, vol. 49, no. 4, pp. 362–370, Dec. 2003.
- [45] S. Bashar, and Z. Ding, “Admission control and resource allocation in a heterogeneous OFDMA wireless network,” *IEEE Trans. Wireless Commun.*, vol. 8, no. 8, pp. 4200–4210, Aug. 2009.
- [46] W. Choi, W. S. Jeon, and D. G. Jeong, “Resource allocation in OFDMA wireless communications systems supporting multimedia services,” *IEEE/ACM Trans. Netw.*, vol. 17, no. 3, pp. 926–935, June 2009.
- [47] K. Seong, M. Mohseni, and J. M. Cioffi, “Optimal resource allocation for OFDMA downlink systems,” *IEEE ISIT 2006, Seattle*, pp. 1394–1398, July 2006.
- [48] C. Y. Wong, R. S. Cheng, K. B. Letaief, and R. D. Murch, “Multiuser OFDM with adaptive subcarrier, bit, and power allocation,” *IEEE J. Sel. Areas Commun.*, vol. 17, no. 10, pp. 1747–1758, Oct. 1999.
- [49] S. Pietrzyk and G. J. M. Janssen, “Multiuser subcarrier allocation for QoS provision in the OFDMA systems,” *Proc. IEEE Veh. Technol. Conf.*, vol. 2, pp. 1077–1081, 2002.
- [50] Y. B. Lin, T. H. Chiu, and Y. Su, “Optimal and near-optimal resource allocation algorithms for OFDMA networks,” *IEEE Trans. Wireless Commun.*, vol. 8, no. 8, pp. 4066–4077, Aug. 2009.
- [51] H. Li, and H. Liu, “An Analysis of Uplink OFDMA Optimality,” *IEEE Trans. Wireless Commun.*, vol. 6, no. 8, pp. 2972–2983, Aug. 2007.
- [52] K. Kim, Y. Han, and S. L. Kim, “Joint subcarrier and power allocation in uplink OFDMA systems,” *IEEE Commun. Lett.*, vol. 9, no. 6, pp. 526–528, June 2005.

- [53] L. Gao, and S. Cui, “Efficient subcarrier, power, and rate allocation with fairness consideration for OFDMA uplink,” *IEEE Trans. Wireless Commun.*, vol. 7, no. 5, pp. 1507–1511, May 2008.
- [54] C. Y. Ng, and C. W. Sung, “Low complexity subcarrier and power allocation for utility maximization in uplink OFDMA systems,” *IEEE Trans. Wireless Commun.*, vol. 7, no. 5, pp. 1667–1675, May 2008.
- [55] G. Li and H. Liu, “Downlink radio resource allocation for multi-cell OFDMA system,” *IEEE Trans. Wireless Commun.*, vol. 5, no. 12, pp. 3451–3459, Dec. 2006.